Earth and Space Science

RESEARCH ARTICLE
10.1029/2023EA003112

Key Points:

- Paleovalley fills are key sediment bodies made up of soft clay, tens of m thick and few km wide, buried beneath coastal lowlands worldwide
- Microtremor-based paleovalley profiles and stratigraphic cross-sections exhibit strong similarity
- Microtremor can provide shear wave velocities and resonance frequencies of paleovalleys, key parameters for seismic hazard mitigation

Correspondence to:
A. Di Martino,
Andrea.dimartino4@unibo.it

Citation:
Di Martino, A., Sgattoni, G., Di Paola, G., Berti, M., & Amorosi, A. (2023). Reconstructing late Quaternary paleovalley systems of Italy through mHVSR: A tool for seismic hazard assessment in modern coastal lowlands. *Earth and Space Science*, *10*, e2023EA003112. https://doi.org/10.1029/2023EA003112

Received 16 JUN 2023
Accepted 12 OCT 2023

Author Contributions:
Conceptualization: Andrea Di Martino, Alessandro Amorosi
Data curation: Andrea Di Martino
Formal analysis: Andrea Di Martino
Funding acquisition: Alessandro Amorosi
Investigation: Andrea Di Martino, Gianluigi Di Paola
Methodology: Giulia Sgattoni
Supervision: Giulia Sgattoni, Matteo Berti, Alessandro Amorosi
Writing – original draft: Andrea Di Martino

Reconstructing Late Quaternary Paleovalley Systems of Italy Through mHVSR: A Tool for Seismic Hazard Assessment in Modern Coastal Lowlands

Andrea Di Martino[1], Giulia Sgattoni[2], Gianluigi Di Paola[3], Matteo Berti[1], and Alessandro Amorosi[1]

[1]Department of Biological, Geological and Environmental Sciences (BiGeA), University of Bologna, Bologna, Italy, [2]Istituto Nazionale di Geofisica e Vulcanologia, Bologna, Italy, [3]ISPRA, Institute for Environmental Protection and Research, ISPRA, Rome, Italy

Abstract Effective site characterization in highly urbanized coastal lowlands requires accurate stratigraphic and geophysical investigations. In these regions, which typically host shallowly buried paleovalley systems formed in response to Quaternary glacio-eustatic fluctuations, the marked lithologic contrast between soft sediment paleovalley fills and the adjacent, stiff substrate has the potential to modify earthquake motions, and assessment of critical parameters, such as shear wave velocities (V_S) and resonance frequencies (f), should be coupled with detailed stratigraphic architecture. To evaluate the potential of the microtremor horizontal-to-vertical spectral ratio (mHVSR) for paleovalley recognition and mapping, we performed mHVSR measurements along the Adriatic coastal plain of Italy, where two paleovalley systems (Pescara and Manfredonia) have been recently identified. In both areas, we detected rapid lateral variations in resonance frequencies and highlighted laterally continuous impedance contrasts. Relying on a robust stratigraphic framework, we carefully evaluated the relation between geological and geophysical data and identified the stratigraphic surfaces responsible for the observed resonances. We derived V_S models for the sediment fill, reconstructing the geometry of the two buried paleovalleys. We address the importance of evaluating the geological context when designing microzonation studies, for a reliable interpretation of changes in resonance frequencies.

Plain Language Summary When earthquakes occur, buildings shake differently based on several factors, including seismic wave velocity, natural resonance frequencies, and local geological characteristics. Beneath modern coastal lowlands, the presence of paleovalley systems can significantly modify the ground motion. Identification of these buried bodies is therefore essential to assess and reduce seismic hazard. Paleovalleys are shallow incisions formed under periods of fluvial erosion in response to Quaternary climate fluctuations, and subsequently filled with very soft clay. These bodies are found worldwide, and do not have any geomorphological evidence, making their recognition challenging. Geologists typically use expensive sediment core analysis to identify paleovalleys, but this method can only provide spotty information. Geophysical exploration techniques that rely on microtremors (small vibrations on the Earth) can complement mapping of these buried bodies. In this work, we tested this technique in Pescara and Mafredonia (Adriatic coastal plain, Italy), providing dense information about paleovalley geometries and geophysical parameters crucial for predicting how the ground will shake during an earthquake. This study also highlights the importance of integrating disciplines to improve our understanding of subsoil and to design future studies to mitigate seismic hazards.

1. Introduction

The prevention of earthquake disasters is an ever-evolving scientific field that relies on contributions from a wide range of disciplines, including civil engineering, geology, and geophysics. Comprehensive site characterization is essential for predicting seismic site effects; it requires accurate reconstruction of subsurface features, including the physical properties of rocks and sediments. In particular, for precise ground motion simulations, shear wave velocities (*Vs*) and resonance frequencies are critical parameters (Chandler et al., 2006; Del Monaco et al., 2013) that should be coupled with detailed three-dimensional modeling of buried stratigraphic architecture.

Writing – review & editing: Giulia Sgattoni, Gianluigi Di Paola, Matteo Berti, Alessandro Amorosi

Delineating lithology and sediment thickness, alongside geophysical and geotechnical properties, is essential in engineering geology, as it plays a critical role in ensuring stable building foundations and understanding local seismic effects (Suopios et al., 2007; Verma et al., 2014) Many site effects studies focus on the vertical 1D characterization of sediment thickness, usually by oversimplifying the lateral variability, while site-specific stratigraphic architecture may significantly influence the frequency content and amplitude of ground motion (Boore, 2004; Hallal & Cox, 2023; Thompson et al., 2009).

The thickness of soft, unconsolidated Quaternary deposits, in particular, may vary significantly in the subsurface of big cities where millions of people live and can dramatically be increased by the presence of buried paleovalley systems.

Late Quaternary paleovalley systems (Blum & Törnqvist, 2000), also known as incised valleys (Van Wagoner et al., 1990), are shallow subsurface incisions formed under prolonged periods of fluvial erosion due to base-level fall, followed by valley filling in response to the rapid sea-level rise (Blum et al., 2013). The paleovalley size is a function of relative sea-level change, water supply, sediment discharge, and local geology and may differ significantly from valley to valley. Paleovalley thickness, typically tens of meters, may exceed 50 m, while width can vary from 2 km to over 15 km (Amorosi et al., 2016, 2023; Campo et al., 2022; Maselli et al., 2014). Paleovalley fills typically have economic value, as they might contain abundant hydrocarbon and water reserves (Dalrymple et al., 1994; Posamentier & Vail, 1988). In addition, these sediment bodies have the potential to modify earthquake ground motion due to their complex lenticular geometry and sharp contrast in geotechnical properties between the very soft clayey fill and generally overconsolidated substrate (Y. Ishihara et al., 2013; Tanabe et al., 2015, 2021).

Late Quaternary paleovalley systems are found worldwide (Anderson et al., 2016; Hori et al., 2023; T. Ishihara & Sugai, 2017; Li et al., 2000), buried beneath modern coastal lowlands and delta plains, and do not have any geomorphological expression; the progressive drowning of the valley, followed by sedimentation above the interfluves, leads to complete obliteration of the primary erosional feature, making paleovalley identification and reconstruction challenging. In Italy, the stratigraphic architecture of late Quaternary paleovalley systems has been documented from the Tyrrhenian Sea coast (Amorosi et al., 2009, 2012, 2013; Milli et al., 2013, 2016), the Ionian Sea coast (Tropeano et al., 2013) and the Adriatic Sea coast (Amorosi et al., 2016, 2017, 2023; Campo et al., 2022; De Santis et al., 2014; Fontana et al., 2008; Maselli & Trincardi, 2013; Maselli et al., 2014; Morelli et al., 2017; Mozzi et al., 2013; Ronchi et al., 2018, 2021). However, detailed geophysical studies and accurate seismic site characterization including resonance frequencies and shear wave velocity of Quaternary paleovalley systems have never been undertaken, so far.

Recently, the Geological Survey of Japan has investigated the physical properties, geometry, and stratigraphic architecture of a Quaternary paleovalley fill beneath the Tokyo and Nakagawa lowlands of the Kanto Plain to mitigate earthquake damage (Y. Ishihara et al., 2013; Tanabe et al., 2015). In this area, paleovalley fills mainly consist of unconsolidated clays, which can amplify seismic waves leading to higher ground shaking (Tanabe et al., 2021). Furthermore, based on data from the 1923 earthquake disaster, Tanabe et al. (2021) established a link between the spatial distribution of the buried paleovalley fill, resonance frequencies, and structural damage to buildings. Reconstructing paleovalley geometries, therefore, is fundamental for a better understanding of seismic site effects.

Buried paleovalley geometries may vary significantly on very short distances (hundreds of m), from the valley flanks (interfluves) to their deepest parts (depocenters) (Amorosi et al., 2023; Campo et al., 2022). Traditional sediment core analysis is a quite expensive exploration tool that can provide detailed lithologic characterization of the valley fill, but no information about its geometry. On the other hand, geophysical investigations, such as shallow seismic imaging and electromagnetic surveys, may be negatively affected by anthropic activities and the presence of large buildings, pipes, and power lines. In this scenario, seismic microtremor surveys, introduced by Aki (1957) and then developed by Okada and Ling (1994) and Okada & Suto (2003), can provide an effective exploration tool. Through microtremor recordings, it is possible to obtain shear wave velocity profiles (Horike, 1985; Köhler et al., 2007; Ohori et al., 2002; Okada & Suto, 2003; Parolai et al., 2005) and also perform the microtremor-based horizontal-to-vertical spectral ratio (mHVSR). The mHVSR method, or simply H/V, was introduced in Japan by Nogoshi and Igarashi (1971) and then popularized by Nakamura (1989, 2000). This geophysical technique is widely used owing to its simplicity and the large amount of information it can provide. In addition, it is widely recognized that the H/V technique offers reliable estimations of the resonance frequency of the surface resonating layer, which is related to sediment thickness, making this technique a fast and powerful

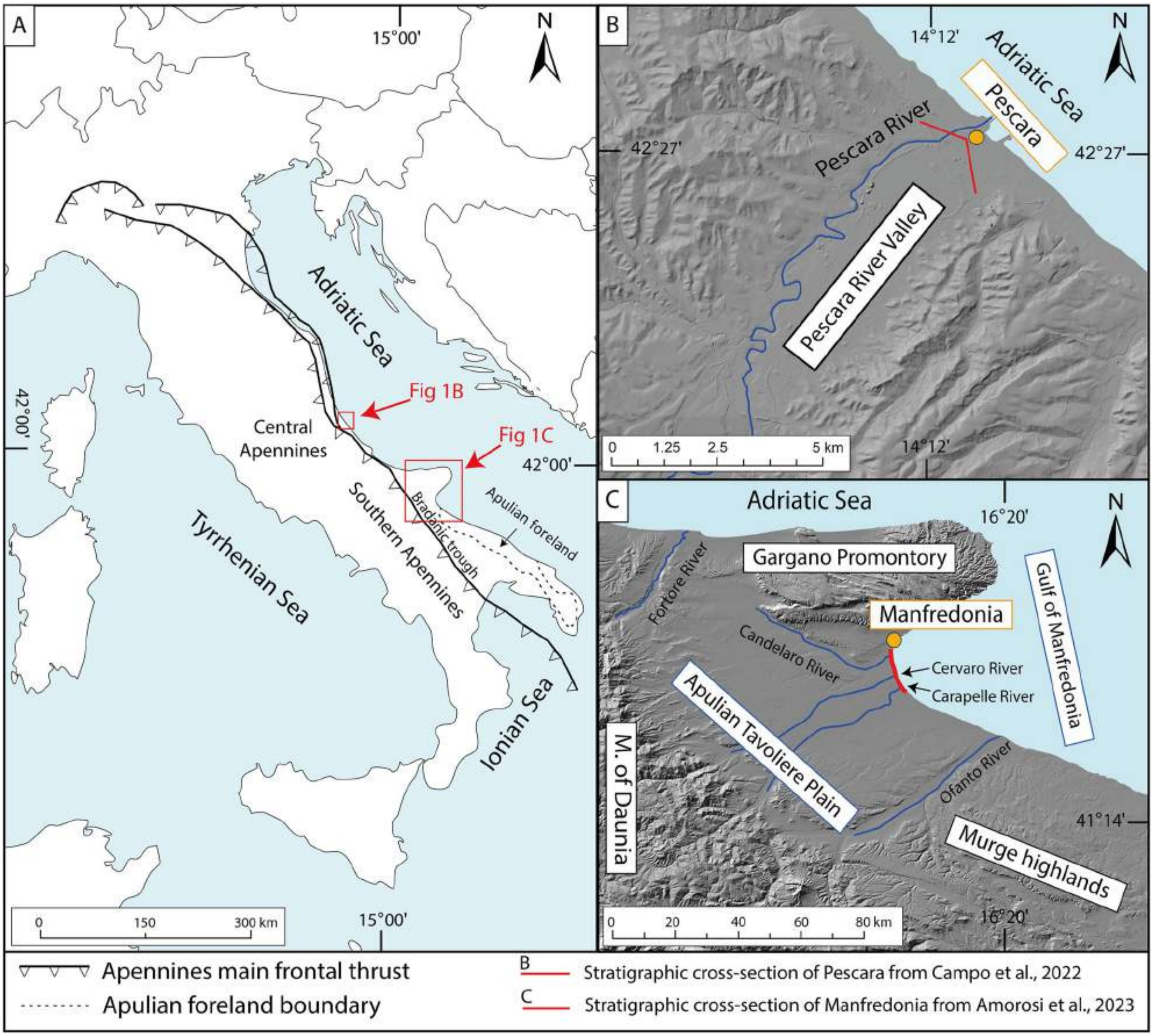

Figure 1. Location of the two study areas (a): the Pescara (b) and Manfredonia (c) coastal lowlands.

stratigraphic tool (e.g., Castellaro & Mulargia, 2009; Grippa et al., 2011; Ibs-von Seht & Wohlenberg, 1999; Parolai et al., 2001, 2002; Sgattoni & Castellaro, 2020, 2021; Tropeano et al., 2011).

To evaluate the potential of mHVSR as an exploration tool for mapping *late* Quaternary paleovalleys, we performed a series of measurements in two areas (Pescara and Manfredonia) along the Adriatic coastal plain of Italy (Figure 1). Here two paleovalley systems have been recently identified and thoroughly described in terms of high-resolution sequence stratigraphy (Amorosi et al., 2023; Campo et al., 2022). Using the robust stratigraphic framework around these sites as a reference and through the acquisition of microtremor measurements along two transects perpendicular to each paleovalley longitudinal axis, the aims of this paper are: (a) to identify variations in resonance frequencies along the transects highlighting laterally continuous impedance contrasts, (b) to carefully evaluate the relation between geological and geophysical data and possibly identify the stratigraphic surfaces responsible for the observed resonances, (c) to derive *Vs* models for the sediment fill in the two paleovalleys, and (d) to estimate the thickness of the soft Holocene valley fills, thus reconstructing the buried paleovalley geometries.

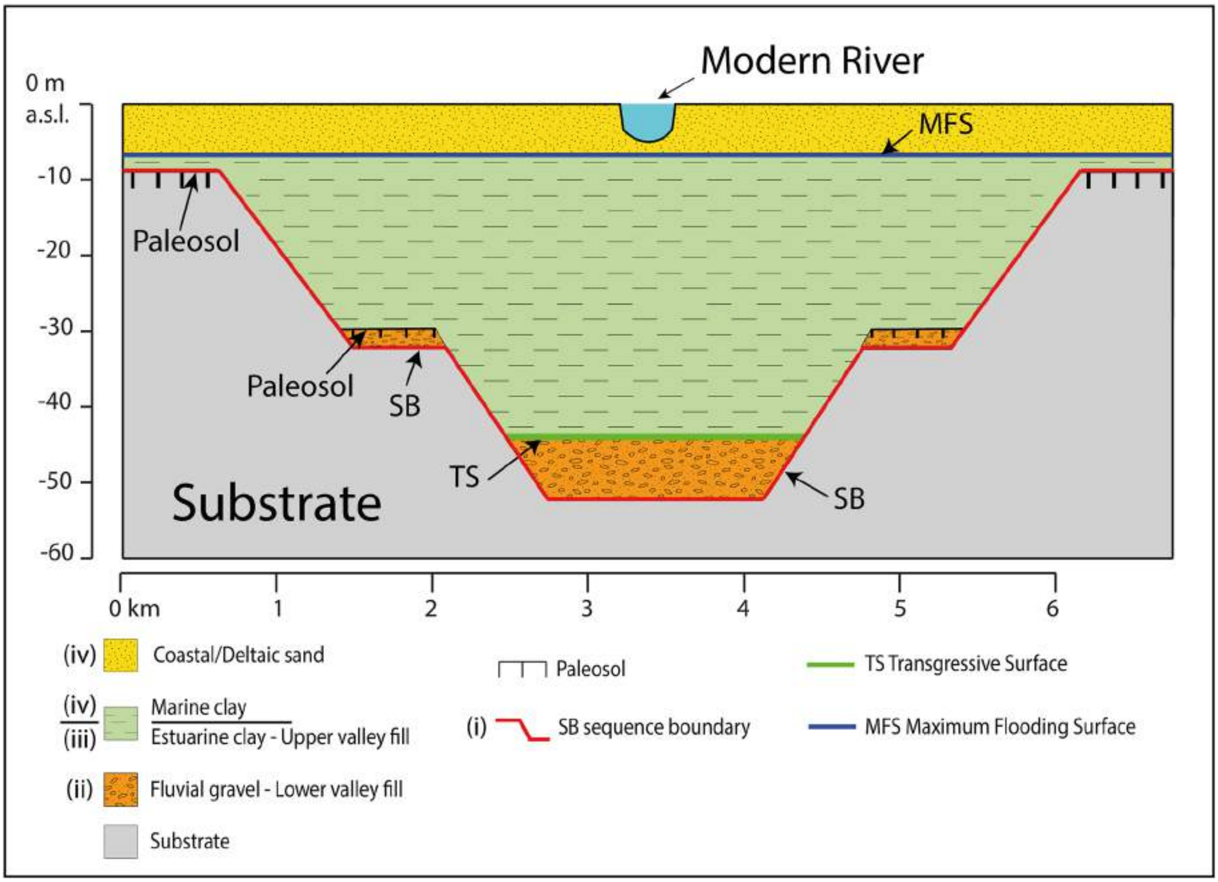

Figure 2. Simplified conceptual paleovalley model, with typical sedimentary fill and key sequence stratigraphic surfaces: sequence boundary, transgressive surface, maximum flooding surface. (i), (ii), (iii), and (iv) refer to the distinct phases of formation and evolution in chapter 2.1.

2. Geological Background

2.1. Paleovalley Systems: Formation, Evolution, and Facies Architecture

Global climate changes, including cyclic variations in ice volume and sea level, controlled the origin and affected the evolution of paleovalley systems during the Quaternary (Blum et al., 2013). Middle to Late Pleistocene paleovalley systems, in particular, display characteristic cycles of erosion and sedimentation (Anderson et al., 2004; Busschers et al., 2007) that reflect glacial-interglacial cycles with a periodicity of ~100 kyr, following the eccentricity of the Earth's orbit. Higher-frequency rhythms predicted by the Milankovitch theory of orbital forcing, including ~43 kyr cyclic changes in axial tilt (Imbrie & Imbrie, 1986; Lisiecki & Raymo, 2007; Martinson et al., 1987; Shackleton & Opdyke, 1973) and ~20 kyr precessional cycles (Prell & Kutzbach, 1992), played a major role in modulating facies architecture of glacial-interglacial depositional cycles. In particular, the late Quaternary paleovalley systems recognized worldwide in the subsurface of modern coastal plains reflect fluvial incision that took place at the transition from Marine Isotope Stages (MIS) 3 to MIS 2 (Amorosi et al., 2017), which was associated with a significant sea-level drop (Lambeck et al., 2014).

The evolution of late Quaternary paleovalleys in the coastal plain exhibits four distinct phases corresponding to a complete cycle of base-level fall and rise (Figure 2):

(i) During period of relative sea-level fall, rivers cut into the substrate, and the valley system shows a degradational pattern with characteristic step-wise incision (Blum et al., 2008; Rittenour et al., 2007). Significant sediment by-pass characterizes the valley in this stage, though fluvial deposits may be preserved locally as alluvial terraces against the valley flanks. The erosional basal valley unconformity is the sequence boundary (SB, Figure 2). In the adjacent interfluves, SB is generally expressed as a paleosol, that is, a soil formed on a past landscape in response to subaerial exposure that was buried subsequently with valley evolution (interfluve SB of Van Wagoner et al. (1990), Aitkien John and Flint Stephen (1996)).

(ii) Under lowstand sea-level conditions, fluvial sedimentation occurs within the valley, forming a characteristic amalgamated gravel or sand body at the valley bottom. This lower valley fill (Blum et al., 2013) is composed of fluvial channels and levee facies representing deposits of migrating and confined channels that cannot avulse outside the paleovalley boundaries (Gibling et al., 2011).

(iii) With relative sea-level rise, valleys are progressively drowned, and fine-grained estuarine facies are deposited above the fluvial deposits, forming the upper valley fill. The transgressive surface (TS, Figure 2), which marks the first significant flooding event (Posamentier & Vail, 1988; Posamentier et al., 1988; Van Wagoner et al., 1990; Zaitlin et al., 1994) separates the gravel or sand fluvial channel-belt from the overlying mud-dominated upper valley fill. Generally, transgressive deposits include a vertical succession of freshwater to brackish estuarine facies formed within the zone of backwater effect during sea-level rise as a landward-tapering wedge (Blum et al., 2013).

(iv) With continuing relative sea-level rise, the valley is filled, the interfluves are drowned, and coastal to shallow-marine environments develop above the paleovalley fill. Above the maximum flooding surface (MFS, Figure 2), which records the maximum marine ingression, prograding coastal and deltaic facies typically cap the succession.

This work expands upon the recent, detailed sedimentological characterization of two paleovalley fills in the Adriatic coastal plain: the Pescara paleovalley (Campo et al., 2022) and the Manfredonia paleovalley (Amorosi et al., 2023). The simplified stratigraphic architecture of these two paleovalley systems is summarized in the following sections.

2.2. The Pescara Paleovalley

The Pescara coastal plain (Figure 1b) in Central Italy is a 3.3 km^2 wide region, narrowly constrained between the Central Apennines and the Adriatic Sea, that hosts the Pescara River mouth. The Pescara River, fed by two main tributaries, Aterno and Sagittario, is the longest river in the Abruzzo region, at over 150 km, and drains a hydrographic basin of about 3,170 km^2 (Urbano et al., 2017).

In the Pescara River valley, a Pliocene-Lower Pleistocene succession of marine deposits, up to 2,000 m thick, is overlain by a Middle Pleistocene-Holocene succession of alluvial deposits in transition to younger coastal facies.

The stratigraphic architecture of the Pescara paleovalley has been recently illustrated by Campo et al. (2022) (Figure 3). The data set (Campo et al., 2022) consists of borehole descriptions down to 45 m depth available from the seismic microzonation project of Pescara Municipality, supplemented by the 52 m-long reference core "Marconi," for which seventeen closely spaced radiocarbon dates are available (Campo et al., 2022). The paleovalley profile and facies architecture were reconstructed based on sedimentological, stratigraphic, geotechnical, and paleontological data. The SB is an erosional surface that marks the abrupt facies change between Lower Pleistocene marine silty clays (Mutignano Fm, and pocket penetrometer value >5 kg/cm^2) and the overlying paleovalley fill. The lower paleovalley fill consists of a laterally extensive, up to 14 m-thick fluvial gravel body accumulated during the Last Glacial Maximum (Figure 3). The basal gravel body is overlain by the upper paleovalley fill of Holocene age, up to 25 m thick, composed of soft (pocket penetrometer values <1 kg/cm^2), organic-rich silty clay accumulated in poorly drained (inner-estuarine) to brackish (outer-estuarine) depositional environments, in response to the post-glacial sea-level rise. The abrupt facies change from fluvial gravels to mud-dominated strata corresponds to the transgressive surface (TS, Figure 3). The upper part of the Holocene succession consists of clay-sand fluvial-deltaic deposits, up to 10 m thick, in lateral transition with coastal sands (Campo et al., 2022).

2.3. The Manfredonia Paleovalley System

In southern Italy, the Apulian Tavoliere coastal plain, about 4,300 km^2 wide, is bounded by two mountain chains and a promontory (Figure 1c): the Daunia Mountains to the west, the Gargano Promontory to the north, and the Murge highlands to the south. It extends north to south for about 90 km, from the Fortore River to the Ofanto River. The Tavoliere is the second-largest alluvial plain in Italy and consists of several Quaternary marine and alluvial terraces (De Santis et al., 2014). Four main rivers drain the modern Tavoliere Plain, from north to south:

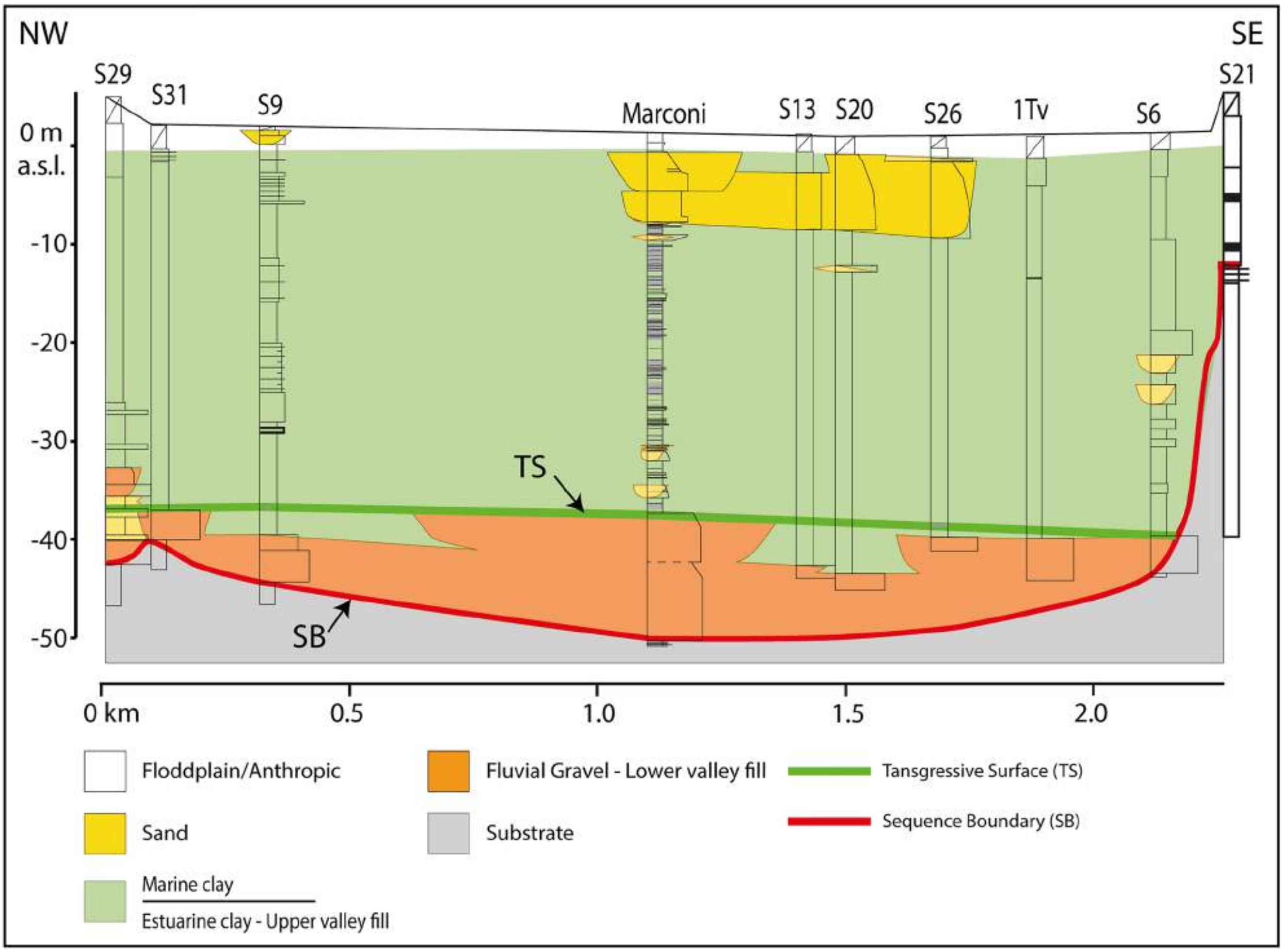

Figure 3. Simplified stratigraphic cross-section of the Pescara paleovalley with vertical exaggeration (Campo et al., 2022). The stratigraphic cross-section is oriented perpendicular to the main paleovalley axis, the trace of the section is shown in Figure 1.

the Candelaro River, 70 km long with a drainage basin (db) of 2,435 km^2, Carapelle River (85 km long, db: 1,465 km^2), Cervaro River (30 km long, db: 625 km^2), and Ofanto River (170 km long, db: 2,780 km^2).

The Gulf of Manfredonia (Figure 1) represents the offshore prolongation of the Tavoliere: it is characterized by a microtidal regime and a sea bottom gently sloping to the east. A laterally extensive unconformity, marking the lower boundary of the Manfredonia paleovalley system related to the Last Glacial Maximum, has been recognized in the subsurface of the Gulf of Manfredonia and in the adjacent offshore areas (De Santis & Caldara, 2016; Maselli & Trincardi, 2013; Maselli et al., 2014; Trincardi et al., 2011). This paleovalley is sinuous and elongated for more than 60 km in a W-E direction, running to the mid-outer shelf. Its onshore prolongation has been recently documented through integrated sedimentological and paleontological analysis of three sediment cores, which enabled the detailed characterization of the stratigraphic architecture of the valley fill (Amorosi et al., 2023 and Figure 4).

The recent stratigraphic analysis of a 50 m-long core from the Manfredonia area, corroborated by 25 radiocarbon data (Amorosi et al., 2023), enabled the reconstruction of the Candelaro paleovalley for example, the onshore part of the “Manfredonia” incised valley identified by Maselli and Trincardi (2013) (Figure 4). The internal anatomy of two adjacent Apulian paleovalleys, generated by the Cervaro and Carapelle rivers (Figure 1c), respectively, was reconstructed based on sedimentological, stratigraphic, geotechnical, paleontological, and geochemical data through a 17-km-long stratigraphic panel (Amorosi et al., 2023 and Figure 4) oriented roughly parallel to the modern shoreline and transversal to the paleovalley axes. Similar to the Pescara paleovalley system, the SB coincides with a prominent erosional stratigraphic surface that truncates older marine strata, indicating a deep fluvial

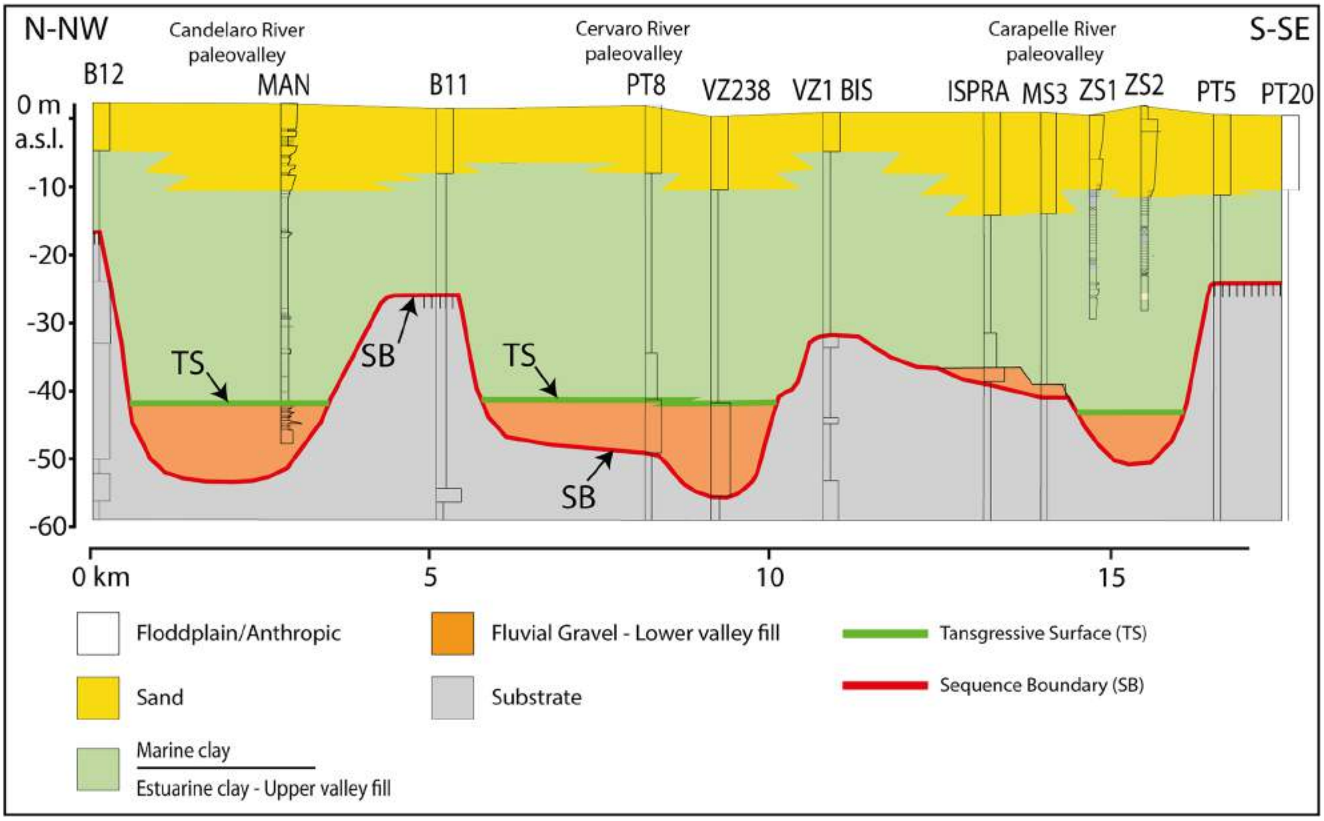

Figure 4. Simplified stratigraphic cross-section of the Candelaro, Cervaro, and Carapelle paleovalley systems in the Manfredonia study area (Amorosi et al., 2023). The stratigraphic section is perpendicular to the paleovalleys axes; the trace of the cross-section is shown in Figure 1.

incision along the major drainage axis. The lower valley fill (Last Glacial Maximum deposits) consists of laterally amalgamated, up to 10 m thick, fluvial-channel gravel and coarse-medium sand that grade upwards into fine to silty sand (Figure 4). Above the fluvial channel sand and gravel, a prominent pedogenized horizon is present, with pocket penetrometer value >6 kg/cm^2. The upper paleovalley fill succession, accumulated in response to the post-glacial sea-level rise, and includes a vertical succession of estuarine and bay deposits, up to 14 m thick, predominantly made of homogeneous silt and clay (pocket penetrometer value <1 kg/cm^2) (Figure 4). The boundary between the sheet-like amalgamated fluvial body and the overlying mud-dominated succession is interpreted as the transgressive surface (TS, Figure 4). Above the paleovalley fill, 12 m thick, unconsolidated marine clay is overlain by 14 m-thick shoreface deposits made predominantly of upward-coarsening sand.

3. Materials and Methods

3.1. HVSR Microtremor Measurements

We collected single-station microtremor recordings (Table 1 and Figure 5) in the Pescara and Manfredonia areas during three field campaigns: in April 2021 and May 2022 for Pescara, and in February 2021 for Manfredonia. All microtremor measurements were carried out using a Tromino® microtremor recorder by MoHo SRL (Italy). This is an all-in-one, three-component velocity/acceleration portable instrument expressly designed to digitally record seismic noise. The sampling rate was 128 Hz, and the acquisition length was 16–30 min, chosen based on the supposed substrate depth inferred by previous stratigraphic studies (Amorosi et al., 2023; Campo et al., 2022) and the local level of anthropic noise. A few measurements were repeated at the same sites with a longer acquisition length to ensure stability of the results.

The instrument was oriented parallel to the geographical North-South direction and leveled on the Earth's surface; sensor leveling and ground stability were maintained throughout the record durations. Coupling the instrument

10.1029/2023EA003112

Table 1
Resonance Frequency and H/V Amplitude of the Microtremor Measurements Acquired for This Study

Pescara			Manfredonia					
Site name	Resonance frequency (Hz)	H/V amplitude (−)	Site name	Resonance frequency (Hz)	H/V amplitude (−)	Site name	Resonance frequency (Hz)	H/V amplitude (−)
P1	3.05 Hz	2	M1	4.50 Hz	3.8	M28	0.95 Hz	3.2
P2	4.03 Hz	2.3	M2	2.97 Hz	3.8	M29	1.05 Hz	2.1
P3	4.20 Hz	3.1	M3	2.46 Hz	4.3	M30	1.1 Hz	2.5
P4	4.30 Hz	3.2	M4	1.62 Hz	2.7	M31	0.94 Hz	2.3
P5	3.8 Hz	4.6	M5	1.62 Hz	2.1	M32	1 Hz	2.8
P6	3.65 Hz	2.3	M6	1.15 Hz	2.1	M33	0.9 Hz	2.6
P7	1.86 Hz	2	M7	0.98 Hz	2.3	M34	0.83 Hz	3
P8	1.58 Hz	2.1	M8	0.92 Hz	2.7	M35	0.86 Hz	2.1
P9	1.24 Hz	1.6	M9	0.91 Hz	3.8	M36	1 Hz	2.3
P10	0.94 Hz	1.6	M10	0.96 Hz	3.9	M37	0.85 Hz	2.3
P11	1.09 Hz	1.7	M11	1.07 Hz	3	M38	1 Hz	2.5
P12	0.97 Hz	1.7	M12	1.14 Hz	2	M39	0.95 Hz	2.4
P13	0.97 Hz	1.8	M13	1.1 Hz	3.2	M40	0.93 Hz	2.3
P14	0.95 Hz	1.9	M14	1.21 Hz	1.5	M41	0.82 Hz	2
P15	1.08 Hz	1.9	M15	1.03 Hz	3.5	M42	0.8 Hz	2
P16	1.23 Hz	1.7	M16	1.06 Hz	2.2	M43	0.82 Hz	1.7
P17	1.14 Hz	1.5	M17	1 Hz	2.3	M44	0.8 Hz	2.1
P18	1.33 Hz	1.5	M18	1.26 Hz	2.3	M45	0.82 Hz	1.7
P19	3.54 Hz	1.6	M19	1.21 Hz	2.1	M46	0.86 Hz	1.6
P20	3.40 Hz	1.9	M20	0.98 Hz	1.9	M47	0.86 Hz	2.3
P21	3.34 Hz	1.8	M21	0.9 Hz	2	M48	0.85 Hz	2.4
P22	3.05 Hz	1.7	M22	0.93 Hz	2.1	M49	1.14 Hz	2
P23	3.56 Hz	1.5	M23	0.88 Hz	3	M50	1.6 Hz	2.5
S18	0.98 Hz	2.3	M24	0.85 Hz	2.9	M51	1.9 Hz	2.4
S19	1.06 Hz	2.6	M25	0.92 Hz	2.7	M52	2.3 Hz	1.3
S24	1.08 Hz	3.8	M26	1 Hz	3.4	M53	2.5 Hz	2.6
S2	1.10 Hz	2.5	M27	1.03 Hz	2.6	M54	2.5 Hz	2.4
S7	1.54 Hz	2.8						
Marconi	1.12 Hz	3.7						

to the Earth's surface is crucial; the sensor feet were firmly inserted into soft soil, vegetation was removed, and the sensor was protected from the direct wind (Chatelain et al., 2008). Although the urban environment presents a challenge to the natural free-field conditions (Castellaro & Mulargia, 2009), we collected all data, avoiding recordings on stiff material over soft soil and at least 15 m away from buildings to minimize their effects (Castellaro & Mulargia, 2010).

The survey was designed to acquire microtremor measurements as close as possible to pre-existing geological data and, where possible, in coincidence with or parallel to the stratigraphic cross-sections of Figures 3 and 4 (see Figure 5 for an overview of all study areas). In Pescara, we acquired 29 mHVSR measurements (Table 1) with about 250 m spacing along an NW-SE oriented, 5 km-long shore-parallel transect crossing the Pescara River (Figure 5a). In Manfredonia, we acquired 54 mHVSR measurements (Table 1), with spacing ranging from 500 to 1,000 m. The recordings were acquired along an NW-SE oriented, 32 km-long shore-parallel transect crossing the Candelaro, Cercaro, and Carapelle rivers (Figure 5b).

10.1029/2023EA003112

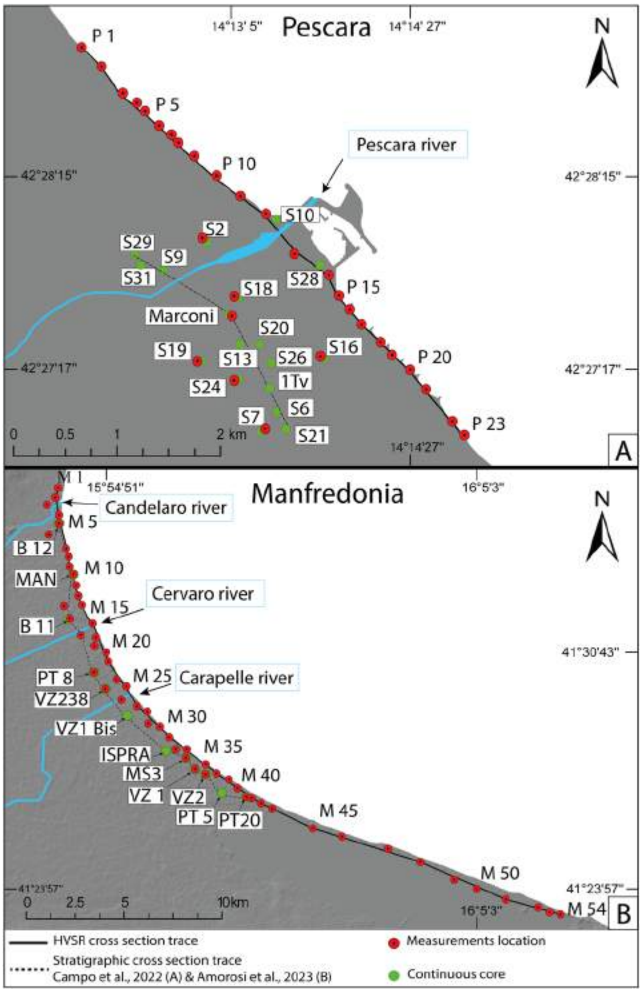

Figure 5. Microtremor measurement locations in Pescara (a) and Manfredonia (b). The black dashed lines represent the two stratigraphic cross-sections of Figures 3 and 4.

3.2. Data Processing

To perform the microtremor-based Horizontal to Vertical Spectral Ratio (mHVSR), we processed the data with the Grilla software. Each three-component time series was split into non-overlapping windows of equal length (30 s). Fourier spectra were computed for each time window and smoothed with triangular functions having a width equal to 10% of the central frequency. We obtained the mHVSR curves by averaging the mHVSR ratios computed for each window, with H being the geometric average of the instrumental N-S and E-W components. The individual spectral components and mHVSR were calculated in terms of average ± standard deviation; transient perturbations were carefully removed by manual selection. To rule out that the results were affected by the chosen processing parameters, a few longer (30 min) recordings were split into longer windows of 60 s, and the results did not change.

3.3. Identification and Lateral Correlation of mHVSR Peaks

The main resonance frequencies of the ground can be identified as distinct peaks on the mHVSR curves, as a function of the depths to the impedance contrasts below the measurement sites. For a correct stratigraphic interpretation, accurate correlation between geological and geophysical data is required. To this aim, we collected all available stratigraphic logs and analyzed our mHVSR curves to check for lateral peak correlation. We analyzed the data in three forms:

(i) Analysis of individual mHVSR curves in conjunction with the spectral components of motion. This type of analysis allows distinguishing the stratigraphic versus anthropic nature of mHVSR peaks (Castellaro, 2016) and discerning the 1D/2D nature of a site (Sgattoni & Castellaro, 2020).
(ii) Lateral plots of mHVSR curves along the investigated lines. These plots allow identifying all mHVSR peaks at all sites, variations between sites, and possibly laterally continuous impedance contrast surfaces.
(iii) Contour plots of mHVSR curves interpolated as a function of distance and color-coded for mHVSR amplitude, with each mHVSR curve individually normalized by its maximum computed within the frequency interval of interest. These plots allow enhancing lateral correlation of the main mHVSR peaks and identification of resonance frequencies associated with common impedance-contrast surfaces.

In Pescara, we identified low-amplitude resonance peaks (mHVSR amplitude mostly around 2) in a frequency range between 1 and 4 Hz. These peaks can be correlated laterally (Figure 6a) to reproduce a U-shaped feature, marked with lower frequencies corresponding to deeper impedance contrasts in the central part of the profile and increasing frequency values toward the edges. A detailed picture of the impedance-contrast surface can be inferred from the contour plot of Figure 6b, where dark-red colors denote the main resonance peaks. In this plot, each mHVSR curve is normalized by its maximum in the frequency range 0.9–4 Hz; by doing this, the detailed frequency features of the maxima associated with the U-shaped surface emerge clearly as a laterally nearly continuous, dark red area and even the smallest lateral frequency variations are visible.

In the Manfredonia area, the mHVSR peaks are more prominent (with amplitudes up to 7) and two distinct resonance peaks characterize several sites. The lateral correlation of these peaks allowed us to identify two different U-shaped features: a relatively shallow impedance contrast at frequencies between 0.9 and 4.5 Hz, and a deeper one at frequencies between about 0.4–1 Hz (Figure 6c). This latter is tentatively associated with the carbonate substrate of Upper Jurassic age expected at 350–400 m depth (Geological Map of Italy, Sheet 409—Zapponeta; Caldara et al., (n.d)). Due to our particular interest in the shallow paleovalley system, which is approximately

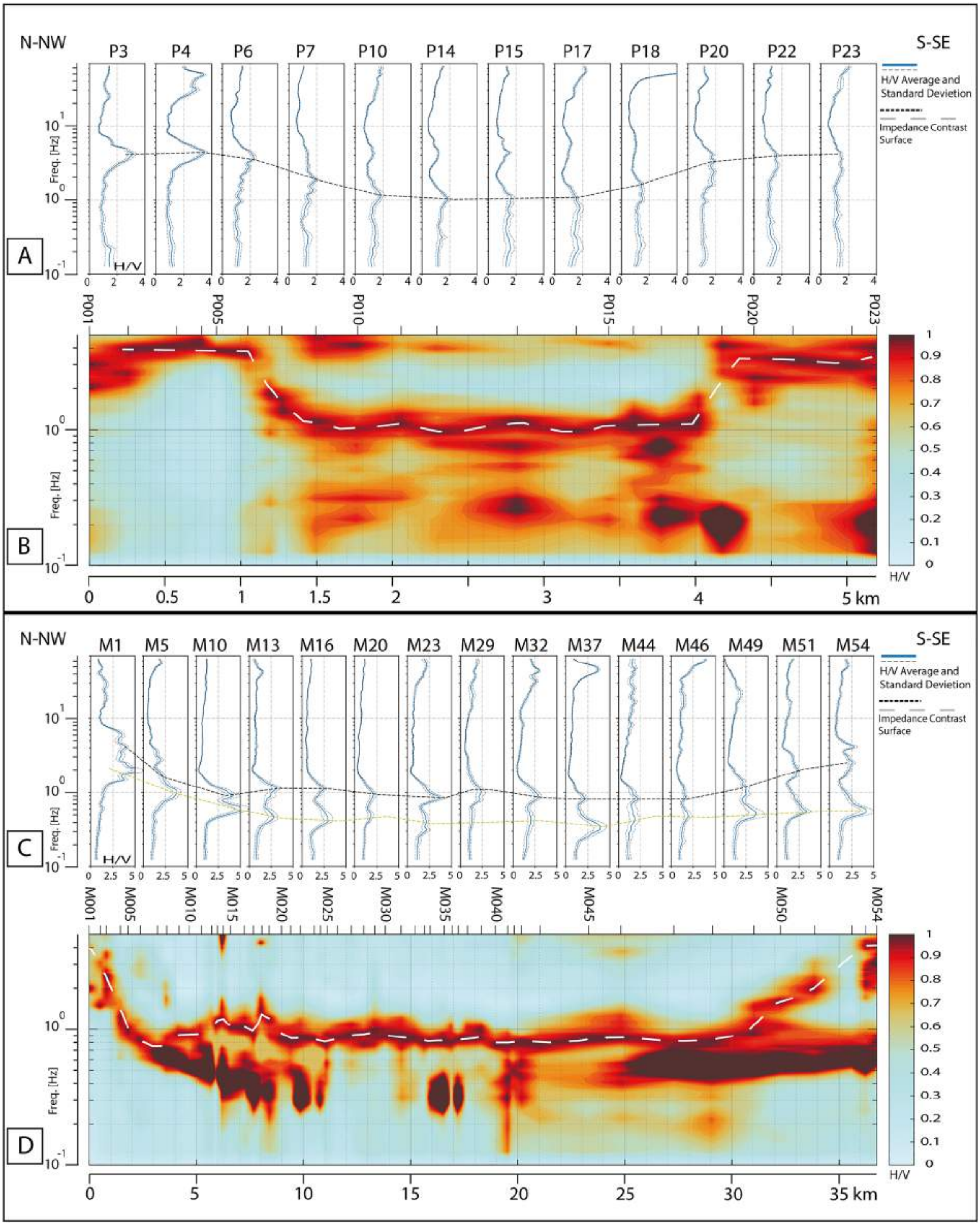

Figure 6. Representative microtremor horizontal-to-vertical spectral ratio (mHVSR) curves of the Pescara (a) and Manfredonia (c) paleovalley systems and complete mHVSR frequency contour plots (b) and (d). The black dashed lines in A and D, and the white dashed lines in B and D, represent the lateral correlation of impedance contrast surface.

50 m deep in its depocenter, we focused further analysis on the shallower layer. The contour plot in Figure 6d shows the resonance frequencies identified along the profile within the frequency range of interest. Here, each mHVSR is individually normalized by its maximum in the frequency range of 0.75–2 Hz.

After inspection of each spectral component of motion, we verified the stratigraphic origin of mHVSR peaks following the criteria described by Castellaro (2016). Most of the resonance peaks are caused by local minima in the vertical spectral components of motion (Figures 7 and 8), a feature related to the lateral propagation of surface waves observed under 1D conditions. The lateral variation of the observed resonance frequencies along the cross-section of both paleovalleys also supports the 1D nature of measurement sites. This suggests that the observed resonance frequency at each site depends on the local stratigraphy and does not represent a 2D vibration mode of the valley fill, which would be reflected in constant resonant frequencies across the valley (Sgattoni & Castellaro, 2020).

3.4. Frequency-To-Depth Conversion

This section describes the procedure to transform the mHVSR profiles from the frequency to the spatial domain. To do this, the 1D resonance equation can be used, which relates the fundamental ground resonance frequency (f_0) with the S-wave velocity (Vs) and thickness (h) of the resonating layer:

$$f_0 = \frac{V_S}{4h} \tag{1}$$

The application of this equation requires (a) the assumption of 1D site conditions at each measurement site, and (b) a Vs model for the sediment layer. The 1D assumption is verified in both study areas for the resonance frequencies of interest (highlighted with white dashed lines in Figure 6). The V_S model can be derived by correlating the observed resonance frequencies with the known depths of impedance contrasts deduced from borehole data (e.g., Ibs-von-Set and Wohlemberg, 1999). To this purpose, we carefully analyzed all microtremor data acquired at nearby sites, where continuous stratigraphic cores are available, and tentatively identified the stratigraphic surfaces that correlate with their corresponding resonance peaks. Four examples of stratigraphic-mHVSR curve correlation are shown in Figures 7 and 8.

In the two paleovalley systems, the depth of the impedance contrast typically coincides with the marked lithologic contrast between the soft, clay-dominated upper paleovalley fill (pocket penetrometer values commonly <1 kg/cm^2) (Figures 7 and 8) and the underlying sand or gravel that typifies the lower valley fill. This major impedance contrast corresponds to the boundary between lowstand fluvial deposits and transgressive estuarine facies (Figure 2). Although it can locally reflect pedogenized horizons (pocket penetrometer value commonly >3 kg/cm^2) at a slightly higher stratigraphic level (core "MAN"—Figure 8), or the direct contact with the substrate (pocket penetrometer value commonly >5 kg/cm^2).

Several HVSR curves from both the Pescara and Manfredonia areas are characterized by mHVSR amplitudes lower than 1 at frequencies higher than about 2 Hz. This feature is typically related to velocity inversions, as described by Castellaro and Mulargia (2009), and is likely due to the shallow stiff sand layer that overlies the soft clay paleovalley fill (Figures 7 and 8).

The resulting frequency-depth constraint points are reported in Figure 9. Here, the column "Substrate depth" generally refers to the depth of the boundary observed locally between the soft, unconsolidated estuarine clay (upper paleovalley fill) and the top of the underlying fluvial gravel (lower paleovalley fill).

A Vs model can be thus derived by fitting resonance frequencies with the identified substrate depths, following the method proposed by Ibs-von Seht and Wohlenberg (1999) that assumes a power-law relation for increasing Vs with depth. This method has been used by numerous authors in several valley contexts (e.g., Paolucci et al., 2015; Parolai et al., 2002; Sgattoni & Castellaro, 2021; Tün et al., 2016; Özalaybey et al., 2011).

The regression analysis was conducted separately for the Pescara paleovalley and the Manfredonia study area, as shown in Figure 9. The frequency-depth relation obtained for the Pescara sediment fill is the following:

$$H = 45.7 f^{-1.26} \tag{2}$$

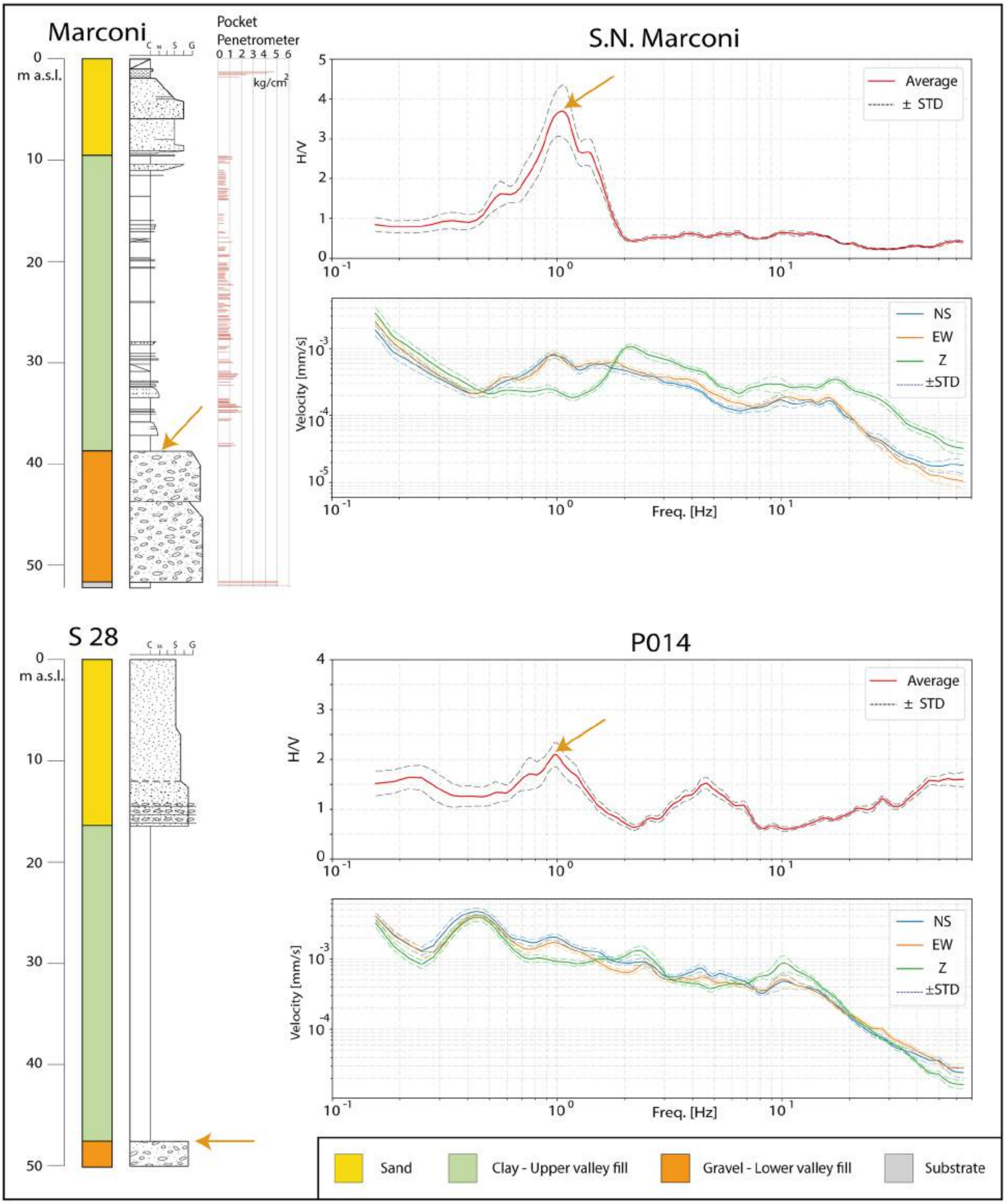

Figure 7. Two cores from the Pescara area, with stratigraphy on the left and related microtremor horizontal-to-vertical spectral ratio measurements with spectra on the right. Pocket penetrometer data from reference core Marconi are shown. Note paleovalley fill values <1 kg/cm^2 and substrate values exceeding 5 kg/cm^2. The orange arrows indicate peaks in the resonance H/V curves and associated impedance contrast surfaces.

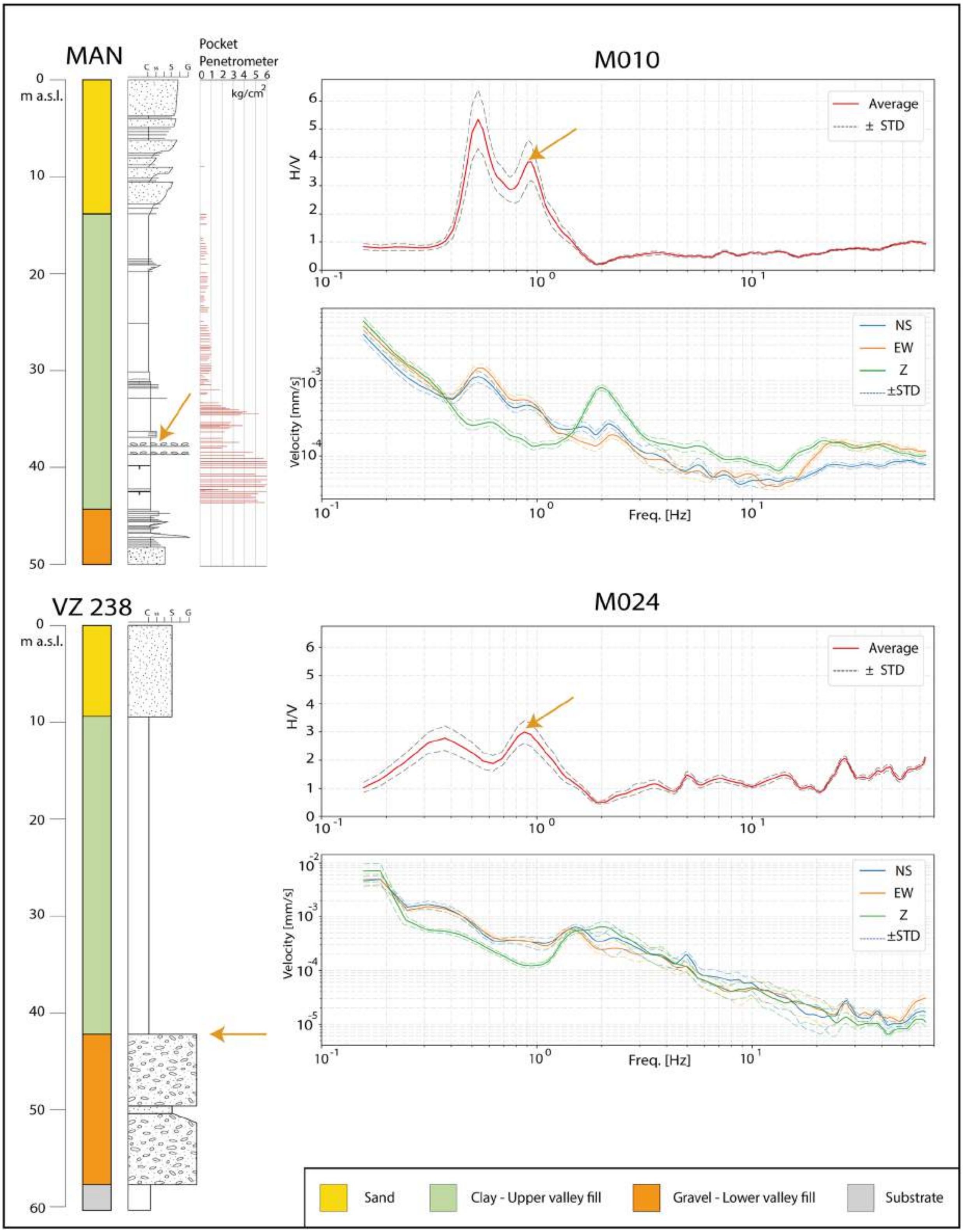

Figure 8. Two cores from the Manfredonia area, with stratigraphy on the left and related microtremor horizontal-to-vertical spectral ratio measurements with spectra on the right. Pocket penetrometer data from reference core MAN are shown. Note paleovalley fill values <1 kg/cm^2 and the pedogenized horizon values >5 kg/cm^2. The orange arrows indicate peaks in the resonance H/V curves and associated impedance contrast surfaces.

10.1029/2023EA003112

Pescara			
Borehole Name	Top of Gravel [m]	H/V Name	Peak frequency [Hz]
S7	26.3	S7	1.5
S16	38.3	P17	1.14
Marconi	39	Marconi	1.12
S2	40.3	S2	1.1
S24	42	S24	1.08
S19	43	S19	1.06
S18	46.5	S18	0.98
S10	47	P12	0.97
S28	49	P14	0.96

Manfredonia			
Borehole	Top of Gravel [m]	H/V name	Peak frequency [Hz]
B12	15	M5	1.7
B11	28.5	M15	1.04
VZ1bis	34	M27/M28	0.94
PT8	36	M22	0.9
MAN	36	M10	0.9
ISPRA	37	M33	0.86
MS3	40	M35	0.83
VZ238	42	M24	0.81

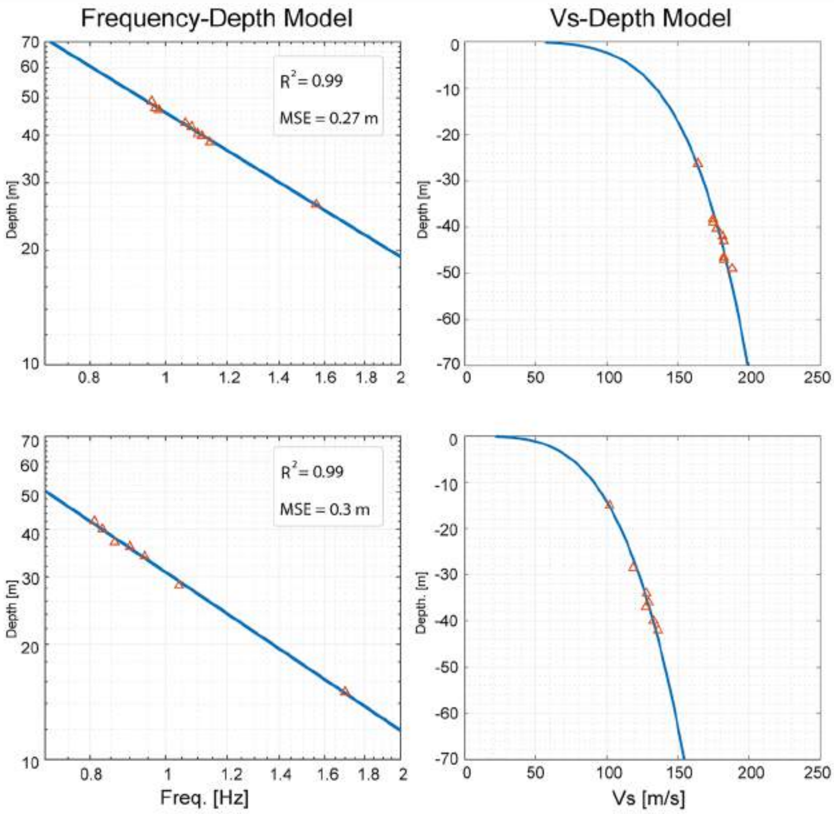

Figure 9. Frequency-depth constraint points for the Pescara and Manfredonia paleovalleys. The two regression models from Equations 2 and 3 and the resulting *Vs*-Depth model are shown.

while for Manfredonia, we obtained:

$$H = 30.8 f^{-1.39} \quad (3)$$

These relations are valid for the shallow subsurface within the depth range used for the regression analysis, which allows the conversion from the frequency to the depth domain of the mHVSR curves.

The data are fitted very well; in both cases, the coefficient of determination R^2 is 0.99, and the mean square error is 0.27 m for the Pescara data set and 0.30 m for Manfredonia. The resulting *Vs* models are also shown in Figure 9. They denote very low *Vs* velocities, with equivalent *Vs* values in the fine-grained paleovalley depocenters, equal to about 180 m/s in Pescara and 140 m/s in Manfredonia.

4. Results

By means of Equations 2 and 3, we transformed the mHVSR curves from the frequency to the spatial domain, down to the base of both paleovalleys. Given the purpose of mapping the shallowly buried paleovalley body, we pushed the reconstructions down to frequencies of approximately 0.9 Hz (corresponding to 50 m) in Pescara and 0.8 Hz (corresponding to 45 m) in Manfredonia. As a result, we obtained two new contour plots, with mHVSR amplitudes as a function of depth and distance along the profiles. Then, we compared the new mHVSR profiles with the corresponding geological cross-sections in Figures 10 and 11.

4.1. The Pescara Paleovalley

In the Pescara area (Figure 10), the stratigraphic cross-section of Figure 3 is parallel to the mHVSR profile, from which it is about 900 m distant. The geological cross-section runs through the Pescara city center, while the

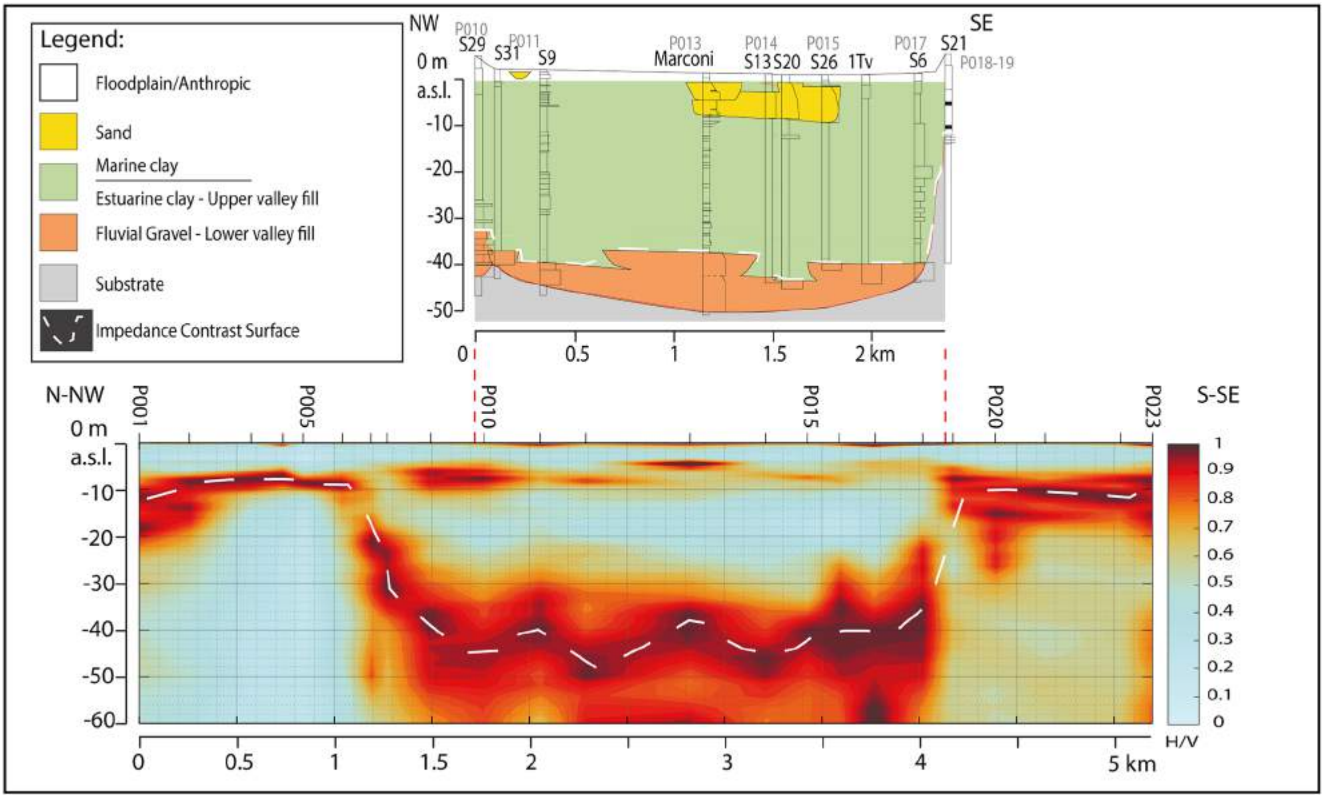

Figure 10. Contour plots of the microtremor horizontal-to-vertical spectral ratio amplitudes function of depth matched against the Pescara geological cross-section. The white dashed lines represent the inferred impedance contrast surfaces.

mHVSR profile runs along the modern Adriatic Sea beach, as shown in Figure 5. The Pescara mHVSR profile is 5.2 km long and extends over a longer distance than the stratigraphic cross-section of the Pescara paleovalley. The stratigraphic transect covers the central portion of the mHVSR profile, approximately from measures P010 to P018 (Figure 10).

From measurements P001 to P006, at approximately 10-m depth, the mHVSR profile shows a clear impedance contrast (Figure 10), interpreted to represent the northern interfluve of the Pescara paleovalley. In this portion of the profile, unconsolidated sand from the modern beach ridge (see section trace in Figure 5) likely overlies the substrate (e.g., Mutignano Fm), producing a high impedance contrast. The fundamental resonance frequency (f_0) of this segment is around 4 Hz and rapidly decreases to 3 Hz at measurement P006 (Figures 6a and 6b).

From measurements P006 to P010, the depth of the impedance contrast surface increases, from 10 to 40 m below sea level (b.s.l.) (Figure 10). In this zone, the fundamental resonance frequency rapidly changes from 3 Hz at P006 to 0.95 Hz at measure P010, within only 700 m distance (Figures 6a and 6b). This area represents the northern flank of the paleovalley. From measurement P010 to P017, the impedance contrast surface stabilizes around 40 m b.s.l. (Figure 10), which is inferred to represent the paleovalley depocenter. In this portion of the profile, minor changes in impedance contrast depth are likely due to the marked thickness variability of the basal gravel body, as shown in the stratigraphic cross-section (Figure 3). In the depocenter, the fundamental resonance frequency is systematically around 1 Hz (Figures 6a and 6b), with some minor changes. For instance, at measure P013, which is almost aligned with core Marconi in the center of the paleovalley, f_0 is 1.17 Hz, consistent with the greater thickness of the fluvial gravel body.

The southern portion of the profile shows an abrupt change in impedance contrast depth from measurement P017 (38 m b.s.l.) to measurement P020 (10 m b.s.l.; Figure 10). A much steeper slope, thus, characterizes the southern flank. From measurement P020 to P023, the depth of the impedance contrast remains stable at approximately 10 m b.s.l.. The sedimentary cover has comparable thickness as in the northern interfluve, as supported by stratigraphic information from core S21. As for the northern interfluve, the dominant resonance frequency varies from 3.5 to 4 Hz (Figures 6a and 6b).

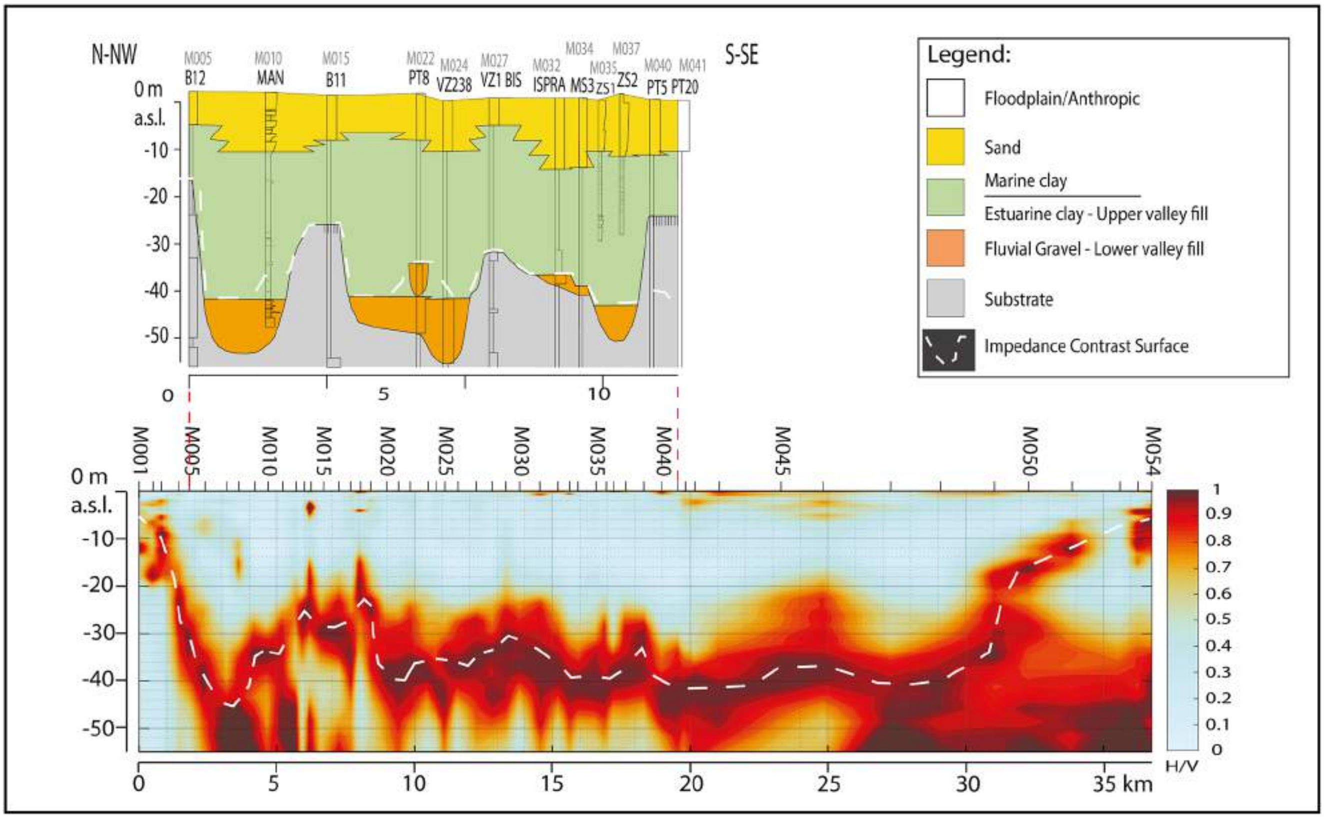

Figure 11. Contour plots of the microtremor horizontal-to-vertical spectral ratio amplitudes function of depth matched against the Manfredonia geological cross-section. The white dashed lines represent the inferred impedance contrast surfaces.

4.2. The Manfredonia Paleovalley

In the Manfredonia area (Figure 11), the internal architecture of three Apulian paleovalleys, generated by the Candelaro, Cervaro, and Carapelle rivers, respectively, is summarized by the 17 km-long stratigraphic cross-section of Figure 4.

Along the Manfredonia mHVSR profile, from measurement M001 to M008, the depth of the impedance contrast surface rapidly increases from 10 m b.s.l. at M001 to 45 m b.s.l. at M008, this latter representing the Candelaro paleovalley depocenter. In this segment, the resonance frequency varies from 4.5 to 0.9 Hz in 3.5 km (Figures 6c and 6d). Between measurements M009-10-11, the impedance contrast surface rises up to 36 m b.s.l. approximately. This change is due to a prominent paleosol observed in the reference core MAN (Figure 8), which coincides with the site where measurement M010 was acquired. From measurement M011 to M019, the impedance surface varies only slightly, from 25 to 30 m b.s.l., with a resonance frequency of around 1.2 Hz (Figures 6c and 6d). Therefore, with core B11 as a support, this zone is interpreted as the interfluve between the Candelaro and Cervaro paleovalleys.

The Cervaro paleovalley was encountered from measurement M020 to M030 (Figure 11), with its depocenter between M022 and M025, consistent with stratigraphic data from cores PT8 and VZ238. In this segment, the depth of the impedance contrast decreases from 41 m b.s.l. (M024), with a resonance frequency of 0.85 Hz–30 m b.s.l. (M030), with a resonance frequency of 1.1 HZ (Figures 6c and 6d), marking a minor interfluve that separates the Cervaro from the Carapelle paleovalleys.

While in the stratigraphic cross-section the Carapelle paleovalley wedges out with its southern interfluve at core PT5 and PT20 (Figure 4), the mHVSR profile does not show the same geometry (Figure 11). Based on the mHVSR profile, the Carapelle paleovalley depocenter would be located, instead, between measurements M040 and M044, with an impedance contrast depth of about 42 m b.s.l. and a resonance frequency of 0.8 Hz (Figures 6c–6d). Such contrasting interpretations likely reflect the low-quality stratigraphic descriptions of cores

PT5 and PT20 on which the geological cross-section is based. The southernmost part of the mHVSR profile has a lower density of measurements and is not supported by stratigraphic information from drillings. Along this transect, the depth of the impedance contrast is systematically low, around 40 m below sea level. Between measurements M048 and M049, the impedance contrast rises up, reaching 10 m b.s.l. at the end of the profile (M054), with a resonance frequency that changes from about 0.8 to 2.5 Hz in 8 km (Figures 6c and 6d), marking the southern interfluve of the paleovalleys system.

5. Discussion and Conclusion

Reconstructing a realistic subsurface stratigraphic model that considers the physical properties of rocks and sediments is fundamental for correct seismic site characterization. In this respect, the mHVSR technique represents a well-known and widely used tool to delineate the subsurface geometry and geophysical properties of the terrain. This method has been successfully applied in diverse geological contexts, including deep valley basins (Ibs-von Seht & Wohlenberg, 1999; Scheib et al., 2016), shallow valley basins, and Alpine valleys (Gosar & Lenart, 2010; Le Roux et al., 2012; Mantovani et al., 2018; Mele et al., 2021; Sgattoni & Castellaro, 2021) and it is also used to investigate weathered rock profiles (Moon et al., 2019), unstable slopes and landslides slip surfaces (Del Gaudio et al., 2014).

Late Quaternary paleovalley systems buried beneath modern coastal lowlands are key geological features for which the efficacy of this geophysical approach is promising due to pronounced lithological contrasts. Paleovalley fills are made up predominantly of very soft, unconsolidated clay with poor geotechnical properties and low shear wave velocities: the combination of these factors may lead to increased structural damage in the event of an earthquake. Nonetheless, reconstructing in detail paleovalley geometries can be expensive, as these buried sediment bodies have no geomorphological expression, and precise identification of depocenters and interfluves in the subsurface requires collection of a large number of sediment cores.

The mHVSR technique proved to be a powerful tool for the subsurface identification of late Quaternary paleovalley systems along the Adriatic Sea coastal plain and an ideal complement to classic stratigraphic reconstructions based on different data sources. The mHVSR profiles from Pescara (Figure 10) and Manfredonia area (Figure 11) show that sharp impedance contrasts can be used effectively to delineate the interfluves of the paleovalley systems and the bases of soft sedimentary valley fills, especially where poor-quality stratigraphic descriptions or absence and scarcity of subsurface data may prevent from reliable stratigraphic reconstructions. This is the case of the southern flank of the Carapelle paleovalley systems in Manfredonia area (Figure 11), where mHVSR data suggest a possibly different interpretation than the one derived from low-quality stratigraphic descriptions, thus contributing significantly to the paleovalley reconstruction.

In general, the mHVSR technique provides a picture of the paleovalley geometry, which is consistent with the one derived from the stratigraphic reconstruction, allowing recognition of important features within the major valley system, such as in the case of the Manfredonia area. The H/V technique not only emphasizes the sharp contrast between the soft clayey valley fill and the underlying gravel but also detects impedance contrasts with prominent paleosols or older (and much more consolidated) substrates. The accurate reconstruction of buried valley geometries can be carried out only through acquisition of a dense network of microtremor measurements: cost-effectiveness and ease of deployment of the mHVSR technique make this approach appropriate for this purpose. Furthermore, the geometries derived from mHVSR reconstructions can be used to plan core drilling campaigns and characterize the paleovalley stratigraphic architecture.

As late Quaternary paleovalley systems have been generated under the global control of glacio-eustatic fluctuations and reflect generalized fluvial incision due to sea-level fall, their worldwide occurrence beneath modern coastal plains and deltas can be predicted in terms of location, size, and geometry. In this regard, the mHVSR technique could be used as a subsurface exploration tool of modern lowlands even where stratigraphic data from drillings are scarce, assuming that basic information on the impedance contrast depth or shear wave velocity is known.

Essential parameters of paleovalley systems other than valley profiles can be obtained through mHVSR investigations. Changes in resonance frequency can be detected by microtremor measurements. In paleovalleys with steep buried flanks, they can vary abruptly without any superficial morphologic evidence in a frequency range that can interact with common building types. In the northern flank of the Pescara paleovalley, the fundamental resonance frequency varies laterally from 3 to 0.9 Hz in only 750 m, remaining stable at 1 Hz in the depocenter (Figures 6a and 6b). Another abrupt variation can be observed along the southern interfluve, where f_0 varies laterally from 0.9 to 3.3 Hz in 600 m only.

The northern portion of the Candelaro paleovalley in the Manfredonia area shows rapid changes in resonance frequencies that vary laterally from 4.5 to 0.9 Hz in 3.5 km (Figures 6c and 6d); other resonance frequency variations can be detected within the main paleovalley body, as part of the minor interfluves separating distinct river domains. For instance, the Candelaro-Cervaro and the Cervaro-Carapelle interfluves are marked by resonance frequency changes from 0.9 Hz to 1.2 and from 0.85 Hz to 1.1, respectively (Figure 4).

In the southern portion of the Manfredonia area, the spacing between mHVSR measurements increases, enabling identification of major resonance frequency changes only and delineating the buried valley morphology, but possibly neglecting local changes that might affect the main paleovalley body, as shown in its northern portion. In this respect, a careful evaluation of the geological context is essential to design an effective microzonation measurements campaign and detect rapid variations in resonance frequencies over short distances, fundamental to preventing building structural damage and can easily be missed in a paleovalley context.

Furthermore, the *Vs* model obtained for the two paleovalleys systems (Figure 9) denotes generally low shear wave velocities, with comparable *Vs* values in the paleovalley depocenters (about 180 m/s in Pescara and 140 m/s in Manfredonia, respectively), placing both paleovalley fills into the ground type D of Standard Eurocode 8, which is a Vs_{30}-based soil classification. Paleovalley geometries and this derived parameter, thus, can be used to improve the quality of local seismic microzonation, and for more accurate site characterization and seismic modeling. In this regard, the shallow velocity inversion due to the uppermost sand layer could also play a role in the seismic response of the paleovalleys, as noted in different contexts, for example, Di Giulio et al. (2016). Further characterization of the velocity model with direct *Vs* measurements would help for exhaustive modeling of the seismic response.

In this study, we utilized the mHVSR technique to reconstruct the geometries of two buried late Quaternary paleovalley systems (Pescara and Manfredonia area) beneath the Adriatic coastal plain of Italy. The microtremor measurements were processed to perform the microtremor-based Horizontal to Vertical Spectral Ratio (mHVSR) and analyzed in conjunction with the spectral components of motion. We recognized clear resonance frequencies in both study areas that outlined the buried valley geometries. Then, assuming a power-law relation for increasing *Vs* with depth and the link between geological and geophysical data, we transformed each mHVSR curve from the frequency to the spatial domain.

We address the importance of integrating geophysical data with accurate stratigraphic reconstructions when performing microzonation studies to ensure reliable geophysical modeling of the critical parameters that control seismic amplification. In paleovalley systems, the resonance frequencies exhibit rapid lateral variation in a range of interactions with standard buildings. The buried paleovalley geometry is typically characterized by steep flanks that can result in 2D seismic effect. Moreover, low S-wave velocities of paleovalley fills can cause longer shaking and seismic amplifications, making this geological context a potential seismic hazard beneath modern coastal lowlands.

Data Availability Statement

The data used for this work are preserved in the repository (AMSacta) hosted by the University of Bologna, Italy, and can be found at the link https://amsacta.unibo.it/id/eprint/7295 (Di Martino et al., 2023). Refer to Table 1 for the name and geographic coordinates of each measure.

Acknowledgments
This research was supported by the Italian Ministry of University and Research under the PRIN 2017 program to Alessandro Amorosi, project number 2017ASZAKJ "The Po-Adriatic Source-to-Sink system (PASS): from modern sedimentary processes to millennial-scale stratigraphic architecture".

References

Aitkien John, F., & Flint Stephen, S. (1996). Variable expressions of interfluvial sequence boundaries in the Breathitt Group (Pennsylvanian), eastern Kentucky, USA. *Geological Society, London, Special Publications*, *104*(1), 193–206. https://doi.org/10.1144/GSL.SP.1996.104.01.12

Aki, K. (1957). Space and time spectra of stationary stochastic waves, with special reference to microtremors. *Bulletin of the Earthquake Research Institute*, *35*, 415–456.

Amorosi, A., Bracone, V., Campo, B., D'Amico, C., Rossi, V., & Rosskopf, C. M. (2016). A late Quaternary multiple paleovalley system from the Adriatic coastal plain (Biferno River, Southern Italy). *Geomorphology*, *254*, 146–159. https://doi.org/10.1016/j.geomorph.2015.11.023

Amorosi, A., Bracone, V., Di Donato, V., Rosskopf, C. M., & Aucelli, P. P. (2009). The Plio-Pleistocene succession between Trigno and Fortore rivers (Molise and Apulia Apennines): Stratigraphy and facies characteristics. *GeoActa*, *8*, 1–12.

Amorosi, A., Bruno, L., Caldara, M., Campo, B., Cau, S., De Santis, V., et al. (2023). Late Quaternary sedimentary record of estuarine incised-valley filling and interfluve flooding: The Manfredonia paleovalley system (southern Italy). *Marine and Petroleum Geology*, *147*, 105975. https://doi.org/10.1016/j.marpetgeo.2022.105975

Amorosi, A., Bruno, L., Campo, B., Morelli, A., Rossi, V., Scarponi, D., et al. (2017). Global sea-level control on local parasequence architecture from the Holocene record of the Po Plain, Italy. *Sedimentology in Italy: Recent Advances and Insights*, *87*, 99–111. https://doi.org/10.1016/j.marpetgeo.2017.01.020

Amorosi, A., Pacifico, A., Rossi, V., & Ruberti, D. (2012). Late Quaternary incision and deposition in an active volcanic setting: The Volturno valley fill, southern Italy. *The 2011 Tohoku-Oki Tsunami*, *282*, 307–320. https://doi.org/10.1016/j.sedgeo.2012.10.003

Amorosi, A., Rossi, V., Sarti, G., & Mattei, R. (2013). Coalescent valley fills from the late Quaternary record of Tuscany (Italy). *Quaternary in Italy: Knowledge and Perspective*, *288*, 129–138. https://doi.org/10.1016/j.quaint.2011.10.015

Anderson, J. B., Rodriguez, A., Abdulah, K. C., Fillon, R. H., Banfield, L. A., McKeown, H. A., & Wellner, J. S. (2004). Late quaternary stratigraphic evolution of the northern Gulf of Mexico margin: A synthesis. In J. B. Anderson & R. H. Fillon (Eds.), *Late quaternary stratigraphic evolution of the northern Gulf of Mexico margin* (Vol. 79). SEPM Society for Sedimentary Geology. https://doi.org/10.2110/pec.04.79.0001

Anderson, J. B., Wallace, D. J., Simms, A. R., Rodriguez, A. B., Weight, R. W. R., & Taha, Z. P. (2016). Recycling sediments between source and sink during a eustatic cycle: Systems of late Quaternary northwestern Gulf of Mexico basin. *Earth-Science Reviews*, *153*, 111–138. https://doi.org/10.1016/j.earscirev.2015.10.014

Blum, M. D., Martin, J. M., Milliken, K. T., & Garvin, M. (2013). Paleovalley systems: Insights from Quaternary analogs and experiments. *Earth-Science Reviews*, *116*, 128–169. https://doi.org/10.1016/j.earscirev.2012.09.003

Blum, M. D., Tomkin, J. H., Purcell, A., & Lancaster, R. R. (2008). Ups and downs of the Mississippi delta. *Geology*, *36*(9), 675–678. https://doi.org/10.1130/G24728A.1

Blum, M. D., & Törnqvist, T. E. (2000). Fluvial responses to climate and sea-level change: A review and look forward. *Sedimentology*, *47*(s1), 2–48. https://doi.org/10.1046/j.1365-3091.2000.00008.x

Boore, D. M. (2004). Can site response be predicted? *Journal of Earthquake Engineering*, *8*(spec01), 1–41. https://doi.org/10.1080/13632460409350520

Busschers, F. S., Kasse, C., van Balen, R. T., Vandenberghe, J., Cohen, K. M., Weerts, H. J. T., et al. (2007). Late Pleistocene evolution of the Rhine-Meuse system in the southern North Sea basin: Imprints of climate change, sea-level oscillation and glacio-isostacy. *Quaternary Science Reviews*, *26*(25), 3216–3248. https://doi.org/10.1016/j.quascirev.2007.07.013

Caldara, M., Capolongo, D., Del Gaudio, V., De Santis, V., Pennetta, L., Maiorano, P., & Simone, O. (n.d.). *Note Illustrative Della Carta Geologica d'Italia alla Scala 1: 50.000 Foglio, 409 "Zapponeta*. Istituto Superiore per la Protezione e la ricerca Ambientale, in press.

Campo, B., Barbieri, G., Di Martino, A., Hong, W., Scarponi, D., Vaiani, S. C., & Amorosi, A. (2022). Late Pleistocene to Holocene glacio-eustatic history as recorded in the Pescara paleovalley system (Central Italy, Adriatic basin). *Marine and Petroleum Geology*, *145*, 105908. https://doi.org/10.1016/j.marpetgeo.2022.105908

Castellaro, S. (2016). The complementarity of H/V and dispersion curves. *Geophysics*, *81*(6), T323–T338. https://doi.org/10.1190/geo2015-0399.1

Castellaro, S., & Mulargia, F. (2009). VS30 estimates using constrained H/V measurements. *Bulletin of the Seismological Society of America*, *99*(2A), 761–773. https://doi.org/10.1785/0120080179

Castellaro, S., & Mulargia, F. (2010). How far from a building does the ground-motion free-field start? The cases of three famous towers and a modern building. *Bulletin of the Seismological Society of America*, *100*(5A), 2080–2094. https://doi.org/10.1785/0120090188

Chandler, A. M., Lam, N. T. K., & Tsang, H. H. (2006). Near-surface attenuation modelling based on rock shear-wave velocity profile. *Soil Dynamics and Earthquake Engineering*, *26*(11), 1004–1014. https://doi.org/10.1016/j.soildyn.2006.02.010

Chatelain, J.-L., Guillier, B., Cara, F., Duval, A.-M., Atakan, K., Bard, P.-Y., & The WP02 SESAME Team. (2008). Evaluation of the influence of experimental conditions on H/V results from ambient noise recordings. *Bulletin of Earthquake Engineering*, *6*(1), 33–74. https://doi.org/10.1007/s10518-007-9040-7

Dalrymple, R. W., Boyd, R., & Zaitlin, B. A. (1994). History of research, types and internal organisation of incised-valley systems: Introduction to the volume. In R. W. Dalrymple, R. Boyd, & B. A. Zaitlin (Eds.), *Incised-valley systems: Origin and sedimentary sequences* (Vol. 51). SEPM Society for Sedimentary Geology. https://doi.org/10.2110/pec.94.12.0003

Del Gaudio, V., Muscillo, S., & Wasowski, J. (2014). What we can learn about slope response to earthquakes from ambient noise analysis: An overview. *Engineering Geology*, *182*, 182–200. https://doi.org/10.1016/j.enggeo.2014.05.010

Del Monaco, F., Tallini, M., De Rose, C., & Durante, F. (2013). HVNSR survey in historical downtown L'Aquila (central Italy): Site resonance properties vs. Subsoil model. *Engineering Geology*, *158*, 34–47. https://doi.org/10.1016/j.enggeo.2013.03.008

De Santis, V., & Caldara, M. (2016). Evolution of an incised valley system in the southern Adriatic Sea (Apulian margin): An onshore–offshore correlation. *Geological Journal*, *51*(2), 263–284. https://doi.org/10.1002/gj.2628

De Santis, V., Caldara, M., Torres, T., & Ortiz, J. E. (2014). Two middle Pleistocene warm stages in the terrace deposits of the Apulia region (southern Italy). *Relative Sea Level Changes: Signature on Continental Shelves, Changing Coastlines, and Implications for Coastal Morphodynamics*, *332*, 2–18. https://doi.org/10.1016/j.quaint.2013.10.009

Di Giulio, G., de Nardis, R., Boncio, P., Milana, G., Rosatelli, G., Stoppa, F., & Lavecchia, G. (2016). Seismic response of a deep continental basin including velocity inversion: The Sulmona intramontane basin (Central Apennines, Italy). *Geophysical Journal International*, *204*(1), 418–439. https://doi.org/10.1093/gji/ggv444

Di Martino, A., Sgattoni, G., Di Paola, G., Berti, M., & Amorosi, A. (2023). HVSR measurements of the Pescara and Manfredonia late quaternary paleovalleys [Dataset]. University of Bologna. https://doi.org/10.6092/UNIBO/AMSACTA/7295

Fontana, A., Mozzi, P., & Bondesan, A. (2008). Alluvial megafans in the Venetian–Friulian Plain (north-eastern Italy): Evidence of sedimentary and erosive phases during Late Pleistocene and Holocene. *Fluvial Architecture and Dynamics in Rising Mountain Chains and Related Basins: Tectonic and Climatic Influences and Human Impacts*, *189*(1), 71–90. https://doi.org/10.1016/j.quaint.2007.08.044

Gibling, M. R., Fielding, C. R., & Sinha, R. (2011). Alluvial valleys and alluvial sequences: Towards a geomorphic assessment. In S. K. Davidson, S. Leleu, & C. P. North (Eds.), *From river to rock record: The preservation of fluvial sediments and their subsequent interpretation* (Vol. 97). SEPM Society for Sedimentary Geology. https://doi.org/10.2110/sepmsp.097.423

Gosar, A., & Lenart, A. (2010). Mapping the thickness of sediments in the Ljubljana Moor basin (Slovenia) using microtremors. *Bulletin of Earthquake Engineering*, *8*(3), 501–518. https://doi.org/10.1007/s10518-009-9115-8

Grippa, A., Bianca, M., Tropeano, M., Cilumbriello, A., Gallipoli, M. R., Mucciarelli, M., & Sabato, L. (2011). Use of the HVSR method to detect buried paleomorphologies (filled incised-valleys) below a coastal plain: The case of the Metaponto plain (Basilicata, southern Italy). *Bollettino di Geofisica Teorica ed Applicata*, *52*(2). https://doi.org/10.4430/bgta0011

Hallal, M. M., & Cox, B. R. (2023). What spatial area influences seismic site response: Insights gained from Multiazimuthal 2D ground response Analyses at the Treasure island downhole Array. *Journal of Geotechnical and Geoenvironmental Engineering*, *149*(1), 04022124. https://doi.org/10.1061/jggefk.gteng-11023

Hori, K., Tanabe, S., & Urabe, A. (2023). Accumulation of thick fluvial sediments in the Shinano River incised-valley fills: Implications for sequence stratigraphy and alluvial architecture. *Journal of Sedimentary Research*, *93*(7), 453–462. https://doi.org/10.2110/jsr.2022.049

Horike, M. (1985). Inversion of phase velocity of long-period microtremors to the S-wave-velocity structure down to the basement in urbanized areas. *Journal of Physics of the Earth*, *33*(2), 59–96. https://doi.org/10.4294/jpe1952.33.59

Ibs-von Seht, M., & Wohlenberg, J. (1999). Microtremor measurements used to map thickness of soft sediments. *Bulletin of the Seismological Society of America*, *89*(1), 250–259. https://doi.org/10.1785/BSSA0890010250

Imbrie, J., & Imbrie, K. P. (1986). *Ice ages: Solving the mystery*. Harvard University Press.

Ishihara, T., & Sugai, T. (2017). Eustatic and regional tectonic controls on late Pleistocene paleovalley morphology in the central Kanto Plain, Japan. *Quaternary International*, *456*, 69–84. https://doi.org/10.1016/j.quaint.2017.06.029

Ishihara, Y., Miyazaki, Y., Eto, C., Fukuoka, S., & Kimura, K. (2013). Shallow subsurface three-dimensional geological model using borehole logs in Tokyo Bay area, central Japan. *The Geological Society of Japan*, *119*(8), 554–566. https://doi.org/10.5575/geosoc.2013.0019

Köhler, A., Ohrnberger, M., Scherbaum, F., Wathelet, M., & Cornou, C. (2007). Assessing the reliability of the modified three-component spatial autocorrelation technique. *Geophysical Journal International*, *168*(2), 779–796. https://doi.org/10.1111/j.1365-246X.2006.03253.x

Lambeck, K., Rouby, H., Purcell, A., Sun, Y., & Sambridge, M. (2014). Sea level and global ice volumes from the last glacial maximum to the Holocene. *Proceedings of the National Academy of Sciences of the United States of America*, *111*(43), 15296–15303. https://doi.org/10.1073/pnas.1411762111

Le Roux, O., Cornou, C., Jongmans, D., & Schwartz, S. (2012). 1-D and 2-D resonances in an Alpine valley identified from ambient noise measurements and 3-D modelling: *1-D and 2-D resonances in an Alpine valley*. *Geophysical Journal International*, *191*(2), 579–590. https://doi.org/10.1111/j.1365-246X.2012.05635.x

Li, C., Chen, Q., Zhang, J., Yang, S., & Fan, D. (2000). Stratigraphy and paleoenvironmental changes in the Yangtze delta during the late quaternary. *Journal of Asian Earth Sciences*, *18*(4), 453–469. https://doi.org/10.1016/S1367-9120(99)00078-4

Lisiecki, L. E., & Raymo, M. E. (2007). Plio–Pleistocene climate evolution: Trends and transitions in glacial cycle dynamics. *Quaternary Science Reviews*, *26*(1), 56–69. https://doi.org/10.1016/j.quascirev.2006.09.005

Mantovani, A., Valkaniotis, S., Rapti, D., & Caputo, R. (2018). Mapping the Palaeo-Piniada valley, central Greece, based on systematic microtremor Analyses. *Pure and Applied Geophysics*, *175*(3), 865–881. https://doi.org/10.1007/s00024-017-1731-7

Martinson, D. G., Pisias, N. G., Hays, J. D., Imbrie, J., Moore, T. C., & Shackleton, N. J. (1987). Age dating and the orbital theory of the ice ages: Development of a high-resolution 0 to 300,000-year chronostratigraphy. *Quaternary Research*, *27*(1), 1–29. Cambridge Core. https://doi.org/10.1016/0033-5894(87)90046-9

Maselli, V., & Trincardi, F. (2013). Large-scale single incised valley from a small catchment basin on the western Adriatic margin (central Mediterranean Sea). *Global and Planetary Change*, *100*, 245–262. https://doi.org/10.1016/j.gloplacha.2012.10.008

Maselli, V., Trincardi, F., Asioli, A., Ceregato, A., Rizzetto, F., & Taviani, M. (2014). Delta growth and river valleys: The influence of climate and sea level changes on the South Adriatic shelf (Mediterranean Sea). *Quaternary Science Reviews*, *99*, 146–163. https://doi.org/10.1016/j.quascirev.2014.06.014

Mele, M., Bersezio, R., Bini, A., Bruno, M., Giudici, M., & Tantardini, D. (2021). Subsurface profiling of buried valleys in central Alps (northern Italy) using HVSR single-station passive seismic. *Journal of Applied Geophysics*, *193*, 104407. https://doi.org/10.1016/j.jappgeo.2021.104407

Milli, S., D'Ambrogi, C., Bellotti, P., Calderoni, G., Carboni, M. G., Celant, A., et al. (2013). The transition from wave-dominated estuary to wave-dominated delta: The Late Quaternary stratigraphic architecture of Tiber River deltaic succession (Italy). *Sedimentary Geology*, *284–285*, 159–180. https://doi.org/10.1016/j.sedgeo.2012.12.003

Milli, S., Mancini, M., Moscatelli, M., Stigliano, F., Marini, M., & Cavinato, G. P. (2016). From river to shelf, anatomy of a high-frequency depositional sequence: The Late Pleistocene to Holocene Tiber depositional sequence. *Sedimentology*, *63*(7), 1886–1928. https://doi.org/10.1111/sed.12277

Moon, S.-W., Subramaniam, P., Zhang, Y., Vinoth, G., & Ku, T. (2019). Bedrock depth evaluation using microtremor measurement: Empirical guidelines at weathered granite formation in Singapore. *Journal of Applied Geophysics*, *171*, 103866. https://doi.org/10.1016/j.jappgeo.2019.103866

Morelli, A., Bruno, L., Cleveland, D. M., Drexler, T. M., & Amorosi, A. (2017). Reconstructing Last Glacial Maximum and Younger Dryas paleolandscapes through subsurface paleosol stratigraphy: An example from the Po coastal plain, Italy. *Geomorphology*, *295*, 790–800. https://doi.org/10.1016/j.geomorph.2017.08.013

Mozzi, P., Ferrarese, F., & Fontana, A. (2013). Integrating digital elevation models and stratigraphic data for the reconstruction of the post-LGM unconformity in the Brenta Alluvial Megafan (North-Eastern Italy). *Alpine and Mediterranean Quaternary*, *26*(1), 41–54.

Nakamura, Y. (1989). A method for dynamic characteristics estimation of subsurface using microtremor on the ground surface. *Railway Technical Research Institute, Quarterly Reports*, *30*(1), 25–33.

Nakamura, Y. (2000). Clear identification of fundamental idea of Nakamura's technique and its applications. In *Proceedings of the 12th World Conference on Earthquake Engineering* (Vol. 2656, pp. 1–8). Retrieved from https://scholar.google.com/scholar?hl=it&as_sdt=0%2C5&q=Clear+identification+of+fundamental+idea+of+Nakamura%E2%80%99s+technique+and+its+applications&btnG=

Nogoshi, M., & Igarashi, T. (1971). On the amplitude characteristics of microtremor, Part II. *Journal of the Seismological Society of Japan*, *24*(1), 26–40. https://doi.org/10.4294/zisin1948.24.1_26

Ohori, M., Nobata, A., & Wakamatsu, K. (2002). A comparison of ESAC and FK methods of estimating phase velocity using arbitrarily shaped microtremor arrays. *Bulletin of the Seismological Society of America*, *92*(6), 2323–2332. https://doi.org/10.1785/0119980109

Okada, H., & Ling, S. Q. (1994). *About a recent study on the surveying geologic structures by using the Microtremor Survey method*. Report of Hokkaido University. Retrieved from https://scholar.google.com/scholar?hl=it&as_sdt=0%2C5&q=Okada%2C+H+Ling+S.Q.++1994+&btnG=#d=gs_cit&t=1675423864596&u=%2Fscholar%3Fq%3Dinfo%3A8s_xPp5vrX8J%3Ascholar.google.com%2F%26output%3Dcite%26scirp%3D0%26hl%3Dit

Okada, H., & Suto, K. (2003). The microtremor survey method. In *Geophysical monograph series*. Society of Exploration Geophysicists (S.E.G.). https://doi.org/10.1190/1.9781560801740.ch3

Özalaybey, S., Zor, E., Ergintav, S., & Tapırdamaz, M. C. (2011). Investigation of 3-D basin structures in the İzmit Bay area (Turkey) by single-station microtremor and gravimetric methods. *Geophysical Journal International*, *186*(2), 883–894. https://doi.org/10.1111/j.1365-246X.2011.05085.x

Paolucci, E., Albarello, D., D'Amico, S., Lunedei, E., Martelli, L., Mucciarelli, M., & Pileggi, D. (2015). A large scale ambient vibration survey in the area damaged by May–June 2012 seismic sequence in Emilia Romagna, Italy. *Bulletin of Earthquake Engineering*, *13*(11), 3187–3206. https://doi.org/10.1007/s10518-015-9767-5

Parolai, S., Bormann, P., & Milkereit, C. (2001). Assessment of the natural frequency of the sedimentary cover in the Cologne area (Germany) using noise measurements. *Journal of Earthquake Engineering*, *05*(04), 541–564. https://doi.org/10.1142/S1363246901000558

Parolai, S., Bormann, P., & Milkereit, C. (2002). New relationships between Vs, thickness of sediments, and resonance frequency calculated by the H/V ratio of seismic noise for the Cologne Area (Germany). *Bulletin of the Seismological Society of America*, *92*(6), 2521–2527. https://doi.org/10.1785/0120010248

Parolai, S., Picozzi, M., Richwalski, S. M., & Milkereit, C. (2005). Joint inversion of phase velocity dispersion and H/V ratio curves from seismic noise recordings using a genetic algorithm, considering higher modes. *Geophysical Research Letters*, *32*(1), L01303. https://doi.org/10.1029/2004GL021115

Posamentier, H. W., Jervey, M. T., & Vail, P. R. (1988). Eustatic Controls on Clastic Deposition I—Conceptual Framework. In C. K. Wilgus, B. S. Hastings, H. Posamentier, J. V. Wagoner, C. A. Ross, & C. G.St. C. Kendall (Eds.), *Sea-level changes: An integrated approach* (Vol. 42). SEPM Special Publication. https://doi.org/10.2110/pec.88.01.0109

Posamentier, H. W., & Vail, P. R. (1988). Eustatic Controls on Clastic Deposition II—Sequence and Systems Tract Models. In C. K. Wilgus, B. S. Hastings, H. Posamentier, J. V. Wagoner, C. A. Ross, & C. G.St. C. Kendall (Eds.), *Sea-level changes: An integrated approach* (Vol. 42). SEPM Special Publication. https://doi.org/10.2110/pec.88.01.0125

Prell, W. L., & Kutzbach, J. E. (1992). Sensitivity of the Indian monsoon to forcing parameters and implications for its evolution. *Nature*, *360*(6405), 647–652. https://doi.org/10.1038/360647a0

Rittenour, T. M., Blum, M. D., & Goble, R. J. (2007). Fluvial evolution of the lower Mississippi River valley during the last 100 ky. Glacial cycle: Response to glaciation and sea-level change. *GSA Bulletin*, *119*(5–6), 586–608. https://doi.org/10.1130/B25934.1

Ronchi, L., Fontana, A., Cohen, K. M., & Stouthamer, E. (2021). Late Quaternary landscape evolution of the buried incised valley of Concordia Sagittaria (Tagliamento River, NE Italy): A reconstruction of incision and transgression. *Geomorphology*, *373*, 107509. https://doi.org/10.1016/j.geomorph.2020.107509

Ronchi, L., Fontana, A., Correggiari, A., & Asioli, A. (2018). Late Quaternary incised and infilled landforms in the shelf of the northern Adriatic Sea (Italy). *Marine Geology*, *405*, 47–67. https://doi.org/10.1016/j.margeo.2018.08.004

Scheib, A., Morris, P., Murdie, R., & Delle Piane, C. (2016). A passive seismic approach to estimating the thickness of sedimentary cover on the Nullarbor Plain, Western Australia. *Australian Journal of Earth Sciences*, *63*(5), 583–598. https://doi.org/10.1080/08120099.2016.1233455

Sgattoni, G., & Castellaro, S. (2020). Detecting 1-D and 2-D ground resonances with a single-station approach. *Geophysical Journal International*, *223*(1), 471–487. https://doi.org/10.1093/gji/ggaa325

Sgattoni, G., & Castellaro, S. (2021). Combining single-station microtremor and gravity surveys for deep stratigraphic mapping. *Geophysics*, *86*(5), G77–G88. https://doi.org/10.1190/geo2020-0757.1

Shackleton, N. J., & Opdyke, N. D. (1973). Oxygen Isotope and Palaeomagnetic Stratigraphy of Equatorial Pacific Core V28-238: Oxygen Isotope Temperatures and Ice Volumes on a 105 Year and 106 Year Scale. *Quaternary Research*, *3*(1), 39–55. Cambridge Core. https://doi.org/10.1016/0033-5894(73)90052-5

Soupios, P. M., Georgakopoulos, P., Papadopoulos, N., Saltas, V., Andreadakis, A., Vallianatos, F., et al. (2007). Use of engineering geophysics to investigate a site for a building foundation. *Journal of Geophysics and Engineering*, *4*(1), 94–103. https://doi.org/10.1088/1742-2132/4/1/011

Tanabe, S., Ishihara, Y., Nakanishi, T., Stafleu, J., & Busschers, F. S. (2021). Distribution of Holocene Marine Mud and its relation to damage from the 1923 earthquake disaster in the Tokyo Metropolitan Area, Japan. *Geosciences*, *11*(7), 272. https://doi.org/10.3390/geosciences11070272

Tanabe, S., Nakanishi, T., Ishihara, Y., & Nakashima, R. (2015). Millennial-scale stratigraphy of a tide-dominated incised valley during the last 14 kyr: Spatial and quantitative reconstruction in the Tokyo Lowland, central Japan. *Sedimentology*, *62*(7), 1837–1872. https://doi.org/10.1111/sed.12204

Thompson, E. M., Baise, L. G., Kayen, R. E., & Guzina, B. B. (2009). Impediments to predicting site response: Seismic property estimation and modeling simplifications. *Bulletin of the Seismological Society of America*, *99*(5), 2927–2949. https://doi.org/10.1785/0120080224

Trincardi, F., Correggiari, A., Ridente, D., Verdicchio, G., Cattaneo, A., Minisini, D., et al. (2011). Carta Geologica dei Mari Italiani. Foglio NK33-8/9 Bari.

Tropeano, M., Cilumbriello, A., Grippa, A., Sabato, L., Bianca, M., Gallicchio, S., et al. (2011). Stratigraphy of the subsurface of the Metaponto Plain vs a geophysical 3D view of the late Pleistocene incised-valleys (Basilicata, Southern Italy). *Rendiconti Online Societa Geologica Italiana*, *17*, 187–193. https://doi.org/10.3301/ROL.2011.54

Tropeano, M., Cilumbriello, A., Sabato, L., Gallicchio, S., Grippa, A., Longhitano, S. G., et al. (2013). Surface and subsurface of the Metaponto Coastal Plain (Gulf of Taranto—Southern Italy): Present-day- vs LGM-landscape. *Continental Shelf Drowned Landscapes (INQUA-CMP and IGCP-526)*, *203*, 115–131. https://doi.org/10.1016/j.geomorph.2013.07.017

Tün, M., Pekkan, E., Özel, O., & Guney, Y. (2016). An investigation into the bedrock depth in the Eskisehir Quaternary Basin (Turkey) using the microtremor method. *Geophysical Journal International*, *207*(1), 589–607. https://doi.org/10.1093/gji/ggw294

Urbano, T., Piacentini, T., & Buccolini, M. (2017). Morphotectonics of the Pescara River basin (Central Italy). *Journal of Maps*, *13*(2), 511–520. https://doi.org/10.1080/17445647.2017.1338204

Verma, M., Singh, R. J., & Bansal, B. K. (2014). Soft sediments and damage pattern: A few case studies from large Indian earthquakes vis-a-vis seismic risk evaluation. *Natural Hazards*, *74*(3), 1829–1851. https://doi.org/10.1007/s11069-014-1283-4

Wagoner, J. C. V., Mitchum, R. M., Campion, K. M., & Rahmanian, V. D. (1990). Siliciclastic Sequence Stratigraphy in Well Logs, Cores, and Outcrops: Concepts for High-Resolution Correlation of Time and Facies. *AAPG Methods in Exploration*, *7*, 3–55. https://doi.org/10.1306/Mth7510

Zaitlin, B. A., Dalrymple, R. W., & Boyd, R. (1994). The Stratigraphic Organization of Incised-Valley Systems Associated with Relative Sea-Level Change. In R. W. Dalrymple, R. Boyd, & B. A. Zaitlin (Eds.), *Incised-valley systems: Origin and sedimentary sequences* (Vol. 51). SEPM Society for Sedimentary Geology. https://doi.org/10.2110/pec.94.12.0045